Adaptive Coding of Face Identity in the Human Visual Cortex

Dissertation submitted for the degree of
Doctor of Philosophy

Petra Hermann

Scientific advisor:

Prof. Zoltán Vidnyánszky, *Ph.D., D.Sc.*

Roska Tamás Doctoral School of Sciences and Technology

Faculty of Information Technology and Bionics

Pázmány Péter Catholic University

Budapest, 2015

"Because I am always interested in faces. I just want you to sit down and look at the human face. But if there is too much going on in the background, if the face moves too much, if you can't see the eyes, if the lighting is too artistic, the face is lost."

(Ingmar Bergman)

Acknowledgements

I would like to express my gratitude for those who accompanied me during my exciting journey. First of all, I would like to say thanks to my supervisor, *Prof. Zoltán Vidnyánszky*, for his support and careful guidance throughout my study and research. *Zoli*, your attitude to scientific thinking and writing makes you a role model for me. I am especially grateful for your trust in me, your attention, patience and impatience as well. I gladly remember our personal discourses about Hantai ("Hantás"). Thank you.

Hereby I also acknowledge the collaborative work and help of *Prof. Gyula Kovács*. *Gyula*, I am particularly thankful to you for the time that I could spend in your lab of Jena.

I am also very grateful to the Doctoral School, especially to *Prof. Tamás Roska* and *Prof. Péter Szolgay* for providing the opportunity to spend my PhD years in a multi-disciplinary environment. I am indebted to *Prof. József Hámori* for his attention and for sharing his educational experiences and abundant knowledge of science and art with me.

I am tremendously thankful to my close tutor colleagues, *Éva Bankó*, *Viktor Gál*, *István Kóbor*, and *Béla Weiss*, for their help, inspiring discussions, and useful advice. *Éva*, I cannot express enough my gratitude for your invaluable scientific and friendly support that I received from you from my first time in the lab. I am very glad that I found a tutor and friend in you. *Viktor*, your grandiose knowledge in MRI methods impressed me and I learned from you that humor is essential in research. Thank you for letting me be part of the "Viktor milieu", and thank you for your friendship.

I am indebted to *Anita Deák* and *Beatrix Lábadi* from the Institute of Psychology of the University of Pécs for encouraging me to take the first steps. *Anita*, I feel enormously grateful to you that I could be part of the fMRI Research Group in Pécs. Thank you for tutoring me and still being my genuine friend up to this day.

Very special thanks to all my fellow PhD students and colleauges in our lab, especially to *Balázs Knakker*, *Vanda Nemes*, *Pál Vakli*, *Petra Kovács*, *Gergely Drótos*, *Regina Meszlényi*, *Ádám Kettinger*, *Máté Kiss*, *Emese Maróti*, *Krisztián Buza*, and *Annamária Manga* for all their help, productive discussions and for the everyday lunch. *Balázs*, we took our first steps in this journey together, sometimes we felt lost, but we could lean on each other and continue our

Contents

Summary of abbreviations

Abbreviation	Concept
3AFC	three-alternative forced-choice
AAL	automated anatomical labeling
ALOI	amsterdam library of objects images
AltB	alternation block
AltT	alternation trial
ANOVA	analysis of variance
aSTS-FA	anterior superior temporal sulcus face area
ATL-FA	anterior temporal lobe face area
BOLD	blood oxygenation level-dependent
CI	confidence interval
CRT	cathode ray tube
D	distance
DCM	dynamic causal modelling
DCT	discrete cosine transform
DLP	digital light processing
EBA	extrastriate body area
EEG	electroencephalography
EPI	echo planar imaging
FC	functional connectivity
FDR	false discovery rate
FFA	fusiform face area
FG	fusiform gyrus
FIE	face inversion effect
fMRI	functional magnetic resonance imaging
fMRIa	functional magnetic resonance imaging adaptation
FWHM	full width at half maximum

Abbreviation	Concept
FOV	field of view
GLM	general linear model
GRE-EPI	gradient-echo echo-planar imaging
HRF	hemodynamic response function
ICBM	international consortium for brain mapping
IF	intact faces or inverted faces
IFG-FA	inferior frontal gyrus face area
IIR	infinite impulse response
IPS	in-plane switching
IT	inferior temporal cortex
LCD	liquid-crystal display
LFP	local field potential
LO or LOC	lateral occipital cortex
MNI	montreal neurological institute
MOG	middle occipital gyrus
MPRAGE	magnetization-prepared rapid gradient-echo
MT+	visual motion area
NF	noisy faces
NO	number of outliers
O	objects
OFA	occipital face area
PC	predictive coding
PCA	principal component analysis
PPI	psychophysiological interaction
pSTS-FA	posterior superior temporal sulcus face area
RepB	repetition block
RepT	repetition trial
ROI	region of interest

Abbreviation	Concept
RS	repetition suppression
rsFC	resting-state functional connectivity
rsfMRI	resting-state functional magnetic resonance imaging
SD	standard deviation
SEM	standard error of the mean
SENSE	sensitivity encoding
SPM	statistical parametric mapping
STS	superior temporal sulcus
TE	echo time
TFE	turbo field echo
TR	repetition time
UF	upright faces

1 Introduction

1.1 Motivations

Face perception is one of the most important functions of the human visual system. Faces convey the majority of socially relevant information, therefore the ability to process faces is essential for normal social functioning. Extensive experimental and modelling research has made significant progress in identifying the neural basis of the remarkably efficient and seemingly effortless face perception in humans. However, the majority of these results might have limited interpretability since they are based on research involving faces that were clear and isolated. On the contrary, in the natural environment, faces occur often under low visibility conditions and/or in rapid succession, thus well-functioning, optimized processing system is needed to enable successful face perception. Uncovering the neural mechanisms underlying face perception in a more realistic context is not only invaluable for a better insight into how visual system works but also could facilitate the development of more efficient training programs on face perception. Furthermore, it could form the basis of more reliable machine-based face recognition algorithms which is a key issue in computer vision.

1.2 How faces are special

The very rich information that is crucial for intact social interaction such as a person's identity, age, gender, expression is conveyed by the face rendering it as a stimulus of exquisite importance. Converging behavioral, neuropsychological, and neuroimaging evidence suggests that faces constitute a special class of visual stimuli with dedicated processing mechanisms that differ from that of other non-face objects (for reviews, see [16, 17]). The most reliable cognitive marker of face-specific processing is the behavioral face inversion effect (FIE, [18]), i.e. the larger drop in performance for faces than for non-face objects due to stimulus inversion (turning the stimulus upside down). Also, accuracy at discriminating individual face parts is higher when they are presented in the context of a face than when presented in isolation, whereas the same holistic advantage is not found for parts of other kinds of stimuli [19]. The double dissociation between face and object processing is known from the neuropsychological literature: patients with prosopagnosia are unable to recognize previously familiar faces, despite a largely preserved ability to recognize objects [20], whereas patients with object-agnosia are seriously impaired in recognizing non-face objects with the spared ability to recognize faces [21]. These results suggest that face perception depends on different neural

processes than those underlying other types of object stimuli. Face-selective areas that were found in the human extrastriate cortex (for reviews, see [16, 22]) might provide the neural substrate for such processes (Fig. 1.1).
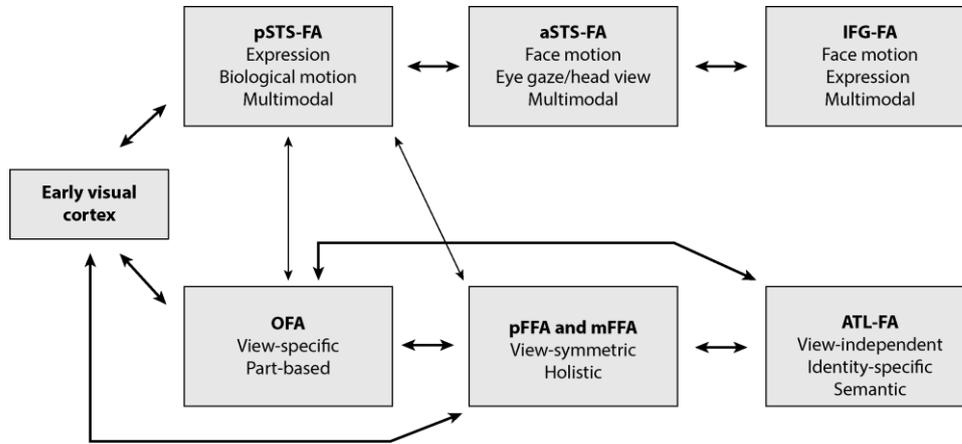
Duchaine B, Yovel G. 2015.
Annu. Rev. Vis. Sci. 1:393–416

Figure 1.1. Revised framework for the roles and connections between face-selective areas. The ventral face-processing pathway consists of the occipital face area (OFA), the fusiform face area (FFA), and the anterior temporal lobe face area (ATL-FA), whereas the dorsal face-processing pathway comprises the posterior superior temporal sulcus face area (pSTS-FA), the anterior superior temporal sulcus face area (aSTS-FA), and the inferior frontal gyrus face area (IFG-FA). (Taken from [16].)

1.3 The fusiform face area (FFA) and its role in face perception

Neuroimaging studies demonstrated that faces elicit robust and selective responses in regions of the human occipital and temporal cortex [23–30] with considerably high reproducibility and reliability in the fusiform gyrus [31]. The region in the mid-fusiform gyrus that consistently shows significantly greater response to faces than to non-face objects has become known as fusiform face area (FFA) [24]. As a central part of the ventral face-processing pathway it has been shown to represent structural, especially temporally invariant properties of faces largely contributing to identity computations [22, 32–36]. The FFA is thought to subserve face perception, since its activity measured with BOLD fMRI was found to be strongly correlated with detection and identification of face images [37–39], and also with the behavioral face inversion effect [40]. However, in these studies face perception was investigated using intact face images, presented without any contextual information. On the contrary, faces that we encounter in real life are often poorly visible due to suboptimal viewing conditions such as insufficient illumination, odd poses etc., and thus their recognition becomes more effortful. In addition, in the majority of social interactions more than two people are engaged and thus it

can dynamically change whose face is in the focus of our attention. To provide efficient communication flow through reacting rapidly and accurately, the visual system must optimize its processing mechanisms under these challenging conditions. An unresolved question is whether FFA maintains its pivotal role in face perception even when face images are noisy or embedded in a temporal context where faces occur in rapid succession.

1.4 Re-entrant mechanisms in the visual system

From a brief glance at a face, we are able to effortlessly assess a person's identity, gender, age, emotional state, and several other characteristics despite the tremendous variation in viewing parameters. This impressive ability of the visual system is mediated by the coordinated computational function of cortical areas involved in face perception [41–44]. Experimental and modeling results suggest that face perception entails an initial, fast categorization of the visual stimulus as a face via rapid feedforward computations along the ventral visual processing stream [45–53] that culminate in a powerful neural face representation in the FFA [30, 54–57]. This early global and coarse face representation is subsequently refined through a re-entrant neural processing loop between the FFA and lower-level visual cortical areas of the inferior and lateral occipital cortex depending on stimulus and task properties [54, 55, 58–61]. It has been suggested [62, 63] that under low visibility conditions the visual system must recruit additional resources to handle the noisy and deteriorated visual image via re-entrant processing mechanisms involving the shape-sensitive lateral occipital cortex (LOC, [64]). Furthermore, when the visual system is put into a continuously changing environment where faces occur in a temporal context, based on short-term prior experience, iterative recurrent mechanisms might help re-estimate and update predictions about sensory input (the same or a different face will be seen), maximizing the efficiency of neural processing, which is supported by the predictive coding model of perception [65–68] (Fig. 1.2). Such processes were suggested to be involved within the core face-processing network composed of the FFA and the occipital face area (OFA, [69]) of the inferior occipital cortex in a DCM study by Ewbank et al. [70]. In sum, the visual system is able to adapt to the challenging conditions of the current environment and provide an accurate perception by optimizing its function, presumably engaging a re-entrant processing loop between higher- and lower-level visual cortical areas. However, the exact neural mechanisms and their relationship to behavior are not yet understood.
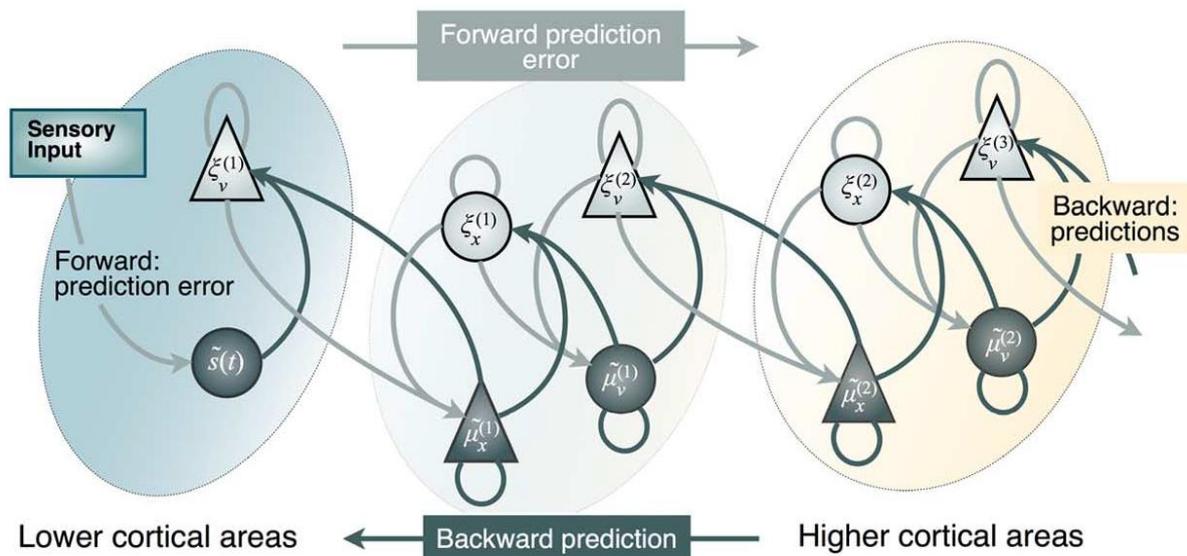
Figure 1.2. One specific example of a recurrent neural network model is the predictive coding model developed by Friston [67]. According to this theory, the brain entails a hierarchical generative model that is used to predict sensory or lower level input. The predictions of the generative model are adjusted at each hierarchical level until the prediction errors between sensory inputs and predictions are minimized. This prediction error minimization process is mediated by forward driving connections, delivering prediction errors (light arrows) from an earlier area to a higher area, and (modulatory) backward connections (dark arrows) that build context-sensitive predictions. (Taken from [71].)

1.5 Predictive coding model of sensory information processing

Predictive coding (PC) theories [65–68] (see [72] for a recent review) consider the brain as an inference engine that actively generates and optimizes probabilistic representations of what caused its sensory input, which results in efficient neuronal information processing. In this framework, one can understand the process of perception as the resolution of sensory prediction errors, by changing top-down predictions about the causes of sensory input (Fig. 1.2). Intuitively, the predictions descending along the cortical processing hierarchy via strong feedback connections are compared against sampled sensory inputs in each hierarchical level of the sensory cortex. The ensuing prediction errors are then passed up the hierarchy to optimize expectations and subsequent predictions identifying the most likely causes of sensory inputs. When the incoming sensory input is noisy, the ascending prediction error will be very imprecise leading to an inaccurate representation and uncertain perceptual decisions [73, 74]. In this case the sensory system must engage additional prediction error minimization processes involving lower-level sensory regions implicated in the processing of low-level high-resolution stimulus features to "explain away" sensory evidence in higher-level regions. However, the direct empirical evidence for such processes is still scarce.

Based on the fact that in real life, the perceptual context tends to be highly stable across short time-scales, prediction is considered to be a fundamental feature of sensory processing in the sense that the initial presentation of the stimulus induces an expectation of that same stimulus reappearing in the near future (for experimental evidence see [75]), maximizing the efficacy of neuronal coding. As a consequence, when a sensory stimulus is repeated, the prediction error is reduced more rapidly as the whole hierarchy settles into a representation of that stimulus, leading to the repetition suppression (RS) of the evoked neural activity [67]. Thus, RS reflects the flexibility of the sensory system and its ability to adjust to continuously changing requirements, optimizing the performance of the individual. Despite the intense effort that has been made to investigate the behavioral advantage of this phenomenon [76–82], the direct link between RS and perceptual ability is not known as of today.

1.6 Goals of the dissertation

The dissertation focuses on how visual cortical processing of faces is affected by the deterioration of image quality and prior perceptual experience. In particular, the research was aimed at:

- uncovering the re-entrant neural processes that enable the extraction of identity information under challenging conditions when face images are deteriorated and noisy.

- revealing the contribution of short-term face adaptation processes mediating the effect of prior experience to face perception.

1.7 Methods

To investigate the above questions, we used traditional task-based and resting-state functional connectivity functional magnetic resonance imaging (fMRI) methods combined with psychophysics. The fMRI is based on the blood oxygenation level-dependent (BOLD) method [83] reflecting signal intensity variations due to blood oxygenation, blood flow, and blood volume changes concomitant with an increase in brain activation. The BOLD fMRI signal, therefore, is a relative and indirect measure of neural activity, which has been shown to strongly correlate with the local field potential (LFP), i.e. a mass neural signal reflecting a multitude of neural processes, including synaptic potentials, afterpotentials of somatodendritic spikes and voltage-gated membrane oscillations [84]. Thus, the BOLD signal in a given brain region is affected by the input of a given cortical area, its local intracortical processing,

including the activity of excitatory and inhibitory interneurons as well as by the activity of neuromodulatory pathways. Over the past decades, fMRI has emerged as the most popular neuroimaging technique used in cognitive neuroscience to study human brain functions. The major advantages of fMRI as compared to other neuroimaging techniques are: non-invasiveness, relatively high spatiotemporal resolution (spatial resolution: 2-3 mm; temporal resolution: 1-3 s) and its capacity to investigate the entire network of brain areas essentially at once either during a particular task or during rest.

1.7.1   Task-based fMRI method

In a standard task-related fMRI analysis experimental factors are manipulated and a general linear model (GLM) is used to identify areas where the activation level associated with one task condition is significantly different from the activation level associated with the other. The contrast between task conditions is carried out separately on the time series for each voxel, which yields a map of contiguous clusters of activated voxels (i.e. statistical parametric maps) forming a set of regions of interest (ROIs) that are assumed to play an important role in generating behavior. A clear dissociation in the foci of activation observed under different task conditions provides strong support for dissociable neural and cognitive mechanisms. In addition, this analysis helps to identify regions that can be used as seeds for more sophisticated subsequent analyses such as for a task-related ROI analysis or an ROI-based intrinsic functional connectivity analysis.

ROI analysis is commonly used to examine activity within a set of functionally coherent voxels, in order to investigate their sensitivity to some other manipulation [85]. This approach is most prevalent in fMRI studies of visual processing, where separate localizers are used to identify functionally specific regions (e.g. voxels in the fusiform gyrus that are more responsive to faces than other objects) for each individual given the large interindividual variability observed in their location in the ventral occipitotemporal cortex [30]. The ROI-based analysis is restricted to voxels of prior interest and, in most cases it involves a univariate amplitude estimation procedure using the GLM approach to examine their response to different task conditions.

1.7.2   Intrinsic functional connectivity fMRI method

The intrinsic functional connectivity fMRI technique has emerged as a powerful non-invasive tool for studying large-scale, spatially distributed networks of the human brain. This method relies on the observation that in the absence of any task, spatially distant regions of cortex exhibit highly correlated spontaneous low-frequency (< 0.1 Hz) fluctuations in their BOLD

signal [86] (see [87] for a review). Resting-state networks are posited to reflect intrinsic representations of functional systems commonly implicated in cognitive function: it has been demonstrated that functional connectivity patterns observed at rest closely correspond to those elicited by more traditional task-based paradigms or derived directly from task data [86, 88–92]. Moreover, growing evidence shows that intrinsic functional connectivity is highly related to task-induced activity [93, 94] and also cognitive ability [95–103] providing support that measuring resting-state connectivity (rsFC) is a useful tool for investigating functionally relevant interactions between cortical areas. One of the most widely adopted method for computing statistical interdependence between brain regions is the univariate seed- or ROI-based functional connectivity analysis where rsFC is represented as a single linear correlation coefficient calculated between 5-15 min time series of a priori ROIs.

1.7.3 Combined fMRI and psychophysics methods

Results of the fMRI experiments demonstrate that a multitude of regions and networks are active during a particular task or rest and show modulation in their activation in a task- or state-dependent manner. Combining fMRI methods with psychophysics, i.e. investigating the relationship between the different fMRI measures (such as task-dependent activity or rsFC) and task performance e.g. by using correlation methods, might provide a more direct and sensitive approach to elucidate the neural mechanisms underlying specific cognitive functions. Furthermore, using this method we can understand how brain function varies across subjects and how these differences relate to the subjects' differences in (separately measured) behavioral performance.

2 Neural basis of identity information extraction from noisy face images

2.1 Introduction

Experimental and modeling results suggest that face perception involves an initial, fast categorization of the visual stimulus as a face (e.g. [45–51, 53]) and it is based primarily on the neural processes in a face-sensitive region in the fusiform gyrus, the fusiform face area (FFA, [24]) [30, 54–57]. This coarse face representation subsequently evolves through re-entrant interactions between the FFA and lower-level visual cortical areas of the inferior and lateral occipital cortex [54, 55, 58–61]. Specifically, in the case of phase-randomized face images, it has been suggested [62, 63] that the increased processing demand due to the distorted spatial localization of the facial features might lead to the engagement of a re-entrant processing loop involving the FFA and a region of the lateral occipital cortex (LOC), which represents shape information within a spatial coordinate system [64, 104] and shows increased fMRI responses to noisy face images [62]. However, an important question that remains to be explored is whether it is the FFA or the LOC on whose neural representations the perception of deteriorated and noisy face images is based. Even though combined behavioral and neuroimaging results provided strong evidence for a close link between face perception and the neural processes in the FFA in the case of intact face images [37–40], it has not been investigated whether this holds true also for faces that are noisy and poorly visible.

To address this question, we measured face identity discrimination performance as well as fMRI responses in the FFA and LOC in the cases of both intact and phase-randomized face stimuli. To examine whether the individual differences in the discrimination of the identity of noisy face stimuli are associated with the noise-induced modulation of fMRI responses in the FFA or in the LOC, we computed correlations between these behavioral and neural measures. Furthermore, based on the suggested role of the re-entrant neural mechanisms in the processing of noisy faces, we predicted that the individual ability to handle stimulus noise might depend on the strength of functional interactions between FFA and LOC. To test this prediction, we estimated the strength of intrinsic functional connectivity between bilateral FFA and LOC using resting-state fMRI [86, 105] (for review, see [87]) and computed correlations between these measures and the face identity discrimination performance for noisy faces.

2.2 Materials and Methods

2.2.1 Subjects

Altogether 26 Caucasian subjects (15 male, 1 left-handed, mean ± SD age: 27 ± 6 years) participated in the experiment and gave informed written consent in accordance with the protocols approved by the ethics committee of Semmelweis University, Budapest, Hungary. None of them had any history of neurological or psychiatric diseases, and all had normal or corrected-to-normal visual acuity.

2.2.2 Psychophysics experiment

Stimuli. In the psychophysics experiment, trials consisted of triplets of morphed male face images. Front-view grayscale images of male faces with neutral expression were cropped to eliminate external features (hair, etc.) and were equated for luminance and contrast. Triplets were obtained by first pairing two individuals and creating a linear morph continuum using a warping algorithm (JPsychoMorph, [106]). Altogether 78 continua were created from 13 individuals. Triplet members were selected from these continua as follows: face A and C were chosen to be the 20/80% and 80/20% points, respectively, while face B was taken from in between, such that the morph distance between the oddball image (e.g. A) and its neighbor (B) was larger than the distance between the other two images (e.g. B and C). These distances were based on pilot measurements to keep performance within the 65-75% range and they differed between face conditions. The following 2 × 2 conditions were used. Faces with 100% phase coherence were presented in the intact face condition, and for the noisy face condition the phase coherence was decreased to 45% (55% noise) (see Fig. 2.1). Phase coherence was manipulated using custom-made scripts based on the weighted mean phase technique [107]. Both intact and noisy faces were presented upright and upside-down.
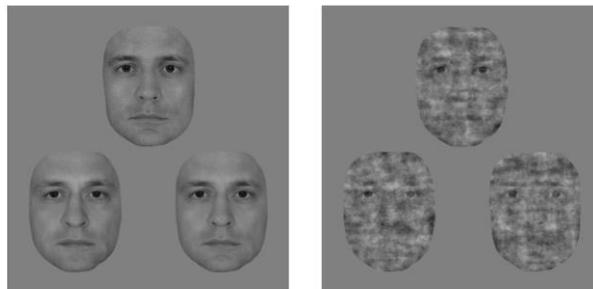

Figure 2.1. Stimuli of the psychophysics experiment. Exemplar face triplet for the intact (left) and the 55% phase noise (right) stimulus condition presented in the 3AFC identity-discrimination task.

Triplets were displayed at the center of the screen on a uniform gray background in a regular triangular arrangement with 4° eccentricity. Triplets measured ~11° × 12°, faces subtending 4.5° × 6.0° each, and were presented on a 26" LG IPS LCD monitor at a refresh rate of 60 Hz viewed from 50 cm. Stimulus presentation was controlled by MATLAB R2010a (The MathWorks Inc., Natick, MA, USA) using the Psychophysics Toolbox Version 3 (PTB-3) [108, 109] (http://psychtoolbox.org/).

Experimental procedure. In the psychophysics experiment, participants performed a three-alternative forced-choice (3AFC) identity fine-discrimination task. Subjects were required to select the face that differed the most from the other two (i.e. oddball face, either A or C). Before the experiment, each subject was given a practice session to get familiar with the task. Each trial began with a cue (1°) appearing just above fixation for 100 ms, indicating the orientation of the upcoming stimuli (upright or inverted). Triplets were presented without a fixation dot under free-viewing conditions until subjects responded, but they were terminated at 5000 ms if no response was made. Trials were separated by an inter-trial interval, which varied randomly between 900 and 1100 ms, with only the fixation dot present. Oddball faces appeared with equal probability in each of the three possible spatial positions. Each unique face triplet was presented only once per condition, randomly assigned to one of the five runs for each participant. Within a single run, the 2 × 2 conditions (intact/noise and upright/inverted) were intermixed and presented in random order. Each participant completed five runs, yielding 65 trials altogether for each condition.

2.3 fMRI experiment

Stimuli. During the block-design fMRI scanning session, images of human faces and common objects were presented. Face stimuli consisted of front-view grayscale photographs of four male faces with neutral, happy, and fearful expressions preprocessed similarly to the images used in the psychophysics experiment. They were presented either with 100% phase coherence (intact face condition) or manipulated by decreasing their phase coherence to 45% (55% noise; noisy face condition) using the weighted mean phase technique [107]. Object stimuli consisted of grayscale images of three different objects from four categories (cars, mugs, jugs, and fruits) chosen from the Amsterdam Library of Objects Images (ALOI) database [110]. All images were equated for luminance and contrast and presented centrally, subtending 4.5° × 6.0°, on a uniform gray background. Stimuli were projected onto a translucent screen located at the back of the scanner bore using a Panasonic PT-D3500E DLP projector (Matsushita Electric Industrial Co., Ltd., Kadoma, Japan) at a refresh rate of 60 Hz, and they were viewed through a mirror attached to the head coil at a viewing distance of 57 cm. Head motion was

minimized using foam padding. Stimulus presentation was controlled by MATLAB R2010a (The MathWorks Inc., Natick, MA, USA) using the Psychophysics Toolbox Version 3 (PTB-3) [108, 109] (http://psychtoolbox.org/).

Experimental procedure. The fMRI session included two block-design runs. In each run, 16 s long blocks of intact faces (IF), noisy faces (NF), and objects (O) were interleaved with baseline blocks which contained only a fixation dot. Stimuli were presented for 500 ms with 0.5 Hz frequency. A run consisted of 6 blocks of each stimulus type (IF, NF, and O) and 19 baseline blocks, making a total number of 37 blocks per run, lasting 10 min each. Subjects performed a one-back memory task and reported the total number of one-back repetitions at the end of the run. In addition to the block-design scans, participants performed an 8 min long resting-state run before the experimental runs. They were instructed to lie still, with their eyes closed.

2.3.1 fMRI scanning

Data were collected at the MR Research Center of Szentágothai Knowledge Center (Semmelweis University, Budapest, Hungary) on a 3 Tesla Philips Achieva scanner (Philips Healthcare, Best, the Netherlands) equipped with an 8-channel SENSE head coil. High-resolution anatomical images were acquired for each subject using a T1-weighted 3D TFE sequence (TR = 9.77 ms, TE = 4.6 ms, FOV = 256 mm) yielding images with $1 \times 1 \times 1$ mm resolution. Functional images were collected with a non-interleaved acquisition order covering the whole brain with a BOLD-sensitive T2*-weighted GRE-EPI sequence. For the experimental fMRI, a total of 301 volumes were acquired using 31 transversal slices (4 mm slice thickness with 3.4 mm $\times$ 3.4 mm in-plane resolution, TR = 2 s, TE = 30 ms, FOV = 220 mm, acceleration factor = 2), while for the resting-state fMRI, a total of 240 volumes were recorded using 36 transversal slices (4 mm slice thickness with 3 mm $\times$ 3 mm in-plane resolution, TR = 2 s, TE = 30 ms, FOV = 240 mm, acceleration factor = 2).

2.3.2 fMRI data analysis

Preprocessing and analysis of the imaging data were performed using the SPM8 toolbox (Wellcome Trust Centre for Neuroimaging, London, UK) and custom MATLAB codes. The functional images were realigned to the first image within a session for motion correction and then spatially smoothed using an 8 mm full width at half maximum (FWHM) Gaussian filter. The anatomical images were coregistered to the mean functional T2*-weighted images followed by segmentation and normalization to the MNI-152 space using SPM's segmentation

toolbox. The gray matter mask was used to restrict statistical analysis on the functional files. To define the regressors for the general linear model analysis of the data, a canonical hemodynamic response function (HRF) was convolved with boxcar functions, representing the onsets of the experimental conditions. Movement-related variance was accounted for by the spatial parameters resulting from the motion correction procedure. A high-pass filter with a cycle-cutoff of 128 s was also implemented in the design to remove low-frequency signals. The prepared regressors were then fitted to the observed functional time series within the cortical areas defined by the gray matter mask. The resulting individual statistical maps were then transformed to the MNI-152 space using the transformation matrices generated during the normalization of the anatomical images. The estimated beta weights of each regressor served as input for the second-level whole-brain random-effects analysis, treating subjects as random factors. For visualization purposes, the IF > NF and NF > IF contrasts were projected with $p_{FDR} < 0.05$ threshold onto the smoothed ICBM152 brain [111–113] using BrainNet Viewer [114] (http://www.nitrc.org/projects/bnv/). Stereotaxic coordinates are reported in Montreal Neurological Institute (MNI) space and regional labels were derived using the AAL atlas [115] provided with XjView 8 (http://www.alivelearn.net/xjview8/).

For the resting-state analysis, several other preprocessing steps were applied in addition to the aforementioned standard preprocessing to reduce spurious variance that is unlikely to reflect neural activity in resting-state data. These steps included voxelwise regression of the time course obtained from rigid-body head motion correction, voxelwise regression of the mean time course of whole-brain, ventricle, and white matter blood oxygen level-dependent (BOLD) fluctuations [116]. To retain low-frequency signals only (0.009–0.08 Hz) [117], we used a combination of temporal high-pass (based on the regression of 9th-order discrete cosine transform (DCT) basis set) and low-pass (bi-directional 12th-order Butterworth IIR) filters.

ROI selection for correlation analysis. We conducted correlation analyses for which we determined the individual locations of three regions of interest (ROIs) (FFA, occipital face area (OFA), and LOC) to take the interindividual variability in their locations into account, which is crucial for intersubject correlations. To define them in each hemisphere and in each participant, we located the peak voxel within a region exhibiting a selective response to face (FFA and OFA) and object images (LOC). The locations of FFA and OFA were determined as the areas in the middle fusiform gyrus and inferior occipital gyrus, respectively, responding more strongly to intact faces than to objects. LOC was identified as the area on the lateral surface of the middle occipital cortex showing significantly stronger activation to objects than to intact faces. Peak voxel activity of all ROIs was required to meet a minimum threshold of $p_{uncorrected} = 0.005$. With each ROI, we took the contiguous cluster of significantly activated

voxels ($t_{(560)} > 2$) within a 10 mm radius sphere centered at the peak voxel and selected a single voxel showing the highest absolute beta difference in the intact versus noisy faces contrast. We used the beta difference (signed to reflect the direction of the contrast) obtained from this voxel to characterize the magnitude of the noise effect in each region for our correlation analysis. The defined voxel coordinates were then transformed to each subject's native space. We only included subjects in the analysis for whom we could individually define these ROIs (for details, see Table 2.1).

ROI	x	y	z	No. of voxels in the cluster	D	N
rFFA	42 ± 0.6	-49 ± 1.0	-21 ± 0.6	253 ± 30	5.2 ± 0.6	23
lFFA	-40 ± 0.7	-49 ± 1.3	-21 ± 0.9	145 ± 34	3.5 ± 0.6	21
rOFA	41 ± 0.7	-76 ± 1.6	-15 ± 0.6	188 ± 31	5.9 ± 0.7	16
rLOC	43 ± 1.0	-78 ± 0.8	9 ± 0.9	167 ± 24	6.6 ± 0.7	18
lLOC	-41 ± 1.0	-80 ± 0.8	7 ± 0.9	229 ± 24	5.8 ± 0.8	19

Table 2.1. Peak voxel coordinates for the regions of interest (ROIs). The MNI coordinates (*x, y, z* in millimeters) of the peak voxels from the IF > O and O < IF contrasts in the case of FFA, OFA, and LOC, respectively. ROIs were defined as the contiguous cluster of significantly activated voxels ($t_{(560)} > 2$) within a 10 mm radius sphere centered at the given peaks. Please note, that for the correlation analysis the activity of a single voxel showing the largest beta difference in the IF versus NF contrast was chosen. The distance (*D*) of this voxel from the peak coordinate of each ROI is also shown in millimeters. Provided data are mean ± SEM across participants (*N*) for whom these regions were individually identifiable. Note that the OFA was reliably definable only in the right hemisphere in the majority of subjects.

For visualization purposes, we generated a probability density map illustrating the spatial distribution of the highest noise effect voxels across participants in the FFA and in the LOC. The individual normalized binary masks for each ROI were first averaged across subjects to create a voxelwise probability map and then convolved it with a 9 mm Gaussian kernel. The kernel size was chosen based on the average distance between the selected voxels of the participants. The resulting voxel density map was superimposed onto the smoothed ICBM152 brain [111–113] using BrainNet Viewer [114] (http://www.nitrc.org/projects/bnv/).

Functional connectivity analysis. To examine functional connectivity at rest, pairwise linear correlations were calculated using the extracted BOLD time course of the predefined ROIs (i.e. the voxel showing the highest noise-related modulation within the ROI) for each

participant. One-sample t tests were performed to determine which regions show reliable resting-state connectivity.

2.3.3 Correlation analysis

To test the behavioral relevance of the noise effect on the fMRI responses, we correlated the individual beta differences in the FFA, OFA, and LOC regions with subjects' discrimination performance on noisy faces. We conducted a semipartial correlation analysis to partial out the influence of the intact face performance on the noisy face accuracy in order to minimize the confounding effect of individual differences in the efficacy of overall face perception of the participants. Skipped Pearson's correlation coefficients were calculated with the Robust Correlation Toolbox [118] in MATLAB. Bivariate outliers were detected using an adjusted box-plot rule and removed in the computation of skipped correlations. For correlation coefficients (r), 95% confidence intervals (CI) were calculated based on 10,000 samples with the percentile bootstrap method implemented in the toolbox.

The relationship between individual resting-state functional connectivity coefficients (rsFC strength) and behavioral performance on noisy faces was studied by computing between-subject partial correlations using skipped Pearson's correlation, eliminating the variance related to efficacy of overall face perception both from the rsFC strength and from the noisy face perception performance. This again served to control for the individual differences in face identity discrimination.

2.4 Results

2.4.1 Behavioral results

The behavioral measures were compared using a two-way repeated-measures ANOVA with within-subject factors of noise (intact vs. noisy face) and inversion (upright vs. inverted face). Face identity discrimination performance was significantly better for intact as compared with noisy faces (main effect of noise: $F_{(1,25)} = 40.95$, $p < 0.001$). Importantly, however, we found robust face inversion effects (i.e. decreased accuracy for inverted faces) for both the intact and noisy face conditions, which did not differ significantly in magnitude (Fig. 2.2; main effect of inversion: $F_{(1,25)} = 72.67$, $p < 0.001$, noise x inversion: $F_{(1,25)} = 0.93$, $p = 0.344$). Thus, noisy face discrimination was based on face-specific processes as opposed to discrimination based

on low-level stimulus features. These behavioral findings suggest that the neural mechanisms involved in the processing of noisy faces might be similar to those of faces without noise.
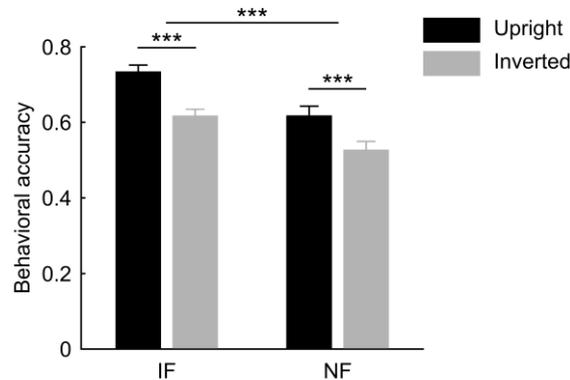
Figure 2.2. Behavioral results. Identity discrimination performance was significantly higher for intact as compared to noisy faces, however face inversion equally impaired accuracy in both cases. Provided data are mean correct response ratio ± SEM across participants (N = 26). Black bars represent data for upright faces; gray bars represent data for inverted faces. IF, intact faces; NF, noisy faces (***$p < 0.001$).

2.4.2   Results of the whole-brain analysis

The whole-brain random-effects analysis of fMRI data using a $p_{FDR} < 0.05$ threshold revealed that the presence of phase noise strongly affected bilateral occipitotemporal cortical processing of face images (Fig. 2.3). To specifically address the questions that we aimed to investigate in the current study, our analysis will be focused on two visual cortical areas: the fusiform gyrus (i.e. FFA) and the middle occipital gyrus (i.e. LOC). Noisy faces relative to intact faces led to decreased activation in the fusiform gyrus bilaterally (Fig. 2.3*A*; $t_{(25)} = 3.83$; *x*, *y*, *z* = 42, −44, −22 and $t_{(25)} = 4.14$; *x*, *y*, *z* = −40, −42, −20 for the right and left hemisphere, respectively), which is in agreement with studies observing noise-induced attenuation in the FFA responses [119–121]. The MNI coordinates of this noise-induced modulation closely corresponds to the mid-fusiform face-selective region referred to as mFus-faces, also known as FFA-2 [29, 122] (for review, see [123]). In contrast, the results also revealed that there was an increased bilateral activation in the middle occipital gyrus in the noisy compared with the intact face condition (Fig. 2.3*B*; $t_{(25)} = 5.18$; *x*, *y*, *z* = 36, −82, 8 and $t_{(25)} = 5.71$; *x*, *y*, *z* = −34, −86, 4 for the right and left hemisphere, respectively), which is in accordance with our previous findings [62]. Based on its coordinates, this region appears to be in close correspondence with the shape-selective, retinotopically organized LO2 area introduced by Larsson and Heeger [64], which is part of the LOC.
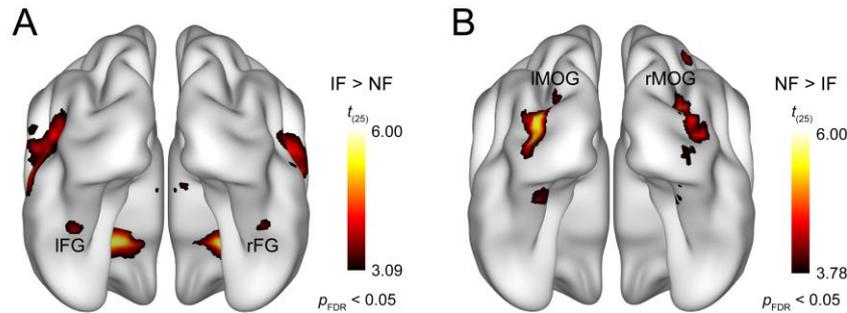
**Figure 2.3.** Results of the whole-brain random-effects analysis. Bilateral areas of the fusiform gyrus showed significantly lower activation for noisy relative to intact faces (*A*), while larger responses to noisy than intact faces were found bilaterally in the middle occipital gyrus (*B*). Statistical maps are displayed with $p_{FDR} < 0.05$ on the smoothed ICBM152 brain [111–113]. IF, intact faces; NF, noisy faces; lFG, left fusiform gyrus; rFG, right fusiform gyrus; lMOG, left middle occipital gyrus; rMOG, right middle occipital gyrus.

2.4.3 Relationship between behavior and fMRI responses to noisy faces

Participants' performance in the three-alternative forced-choice identity discrimination task was $73.8 \pm 1.7\%$ and $61.9 \pm 1.7\%$ (mean $\pm$ SEM) in the case of intact and phase-randomized face stimuli, respectively. To investigate the relationship between the noise-induced modulation found in the fMRI responses and individual performance to noisy faces, we conducted a semipartial correlation analysis using the intact face performance as a covariate for the noisy face performance to control for the confounding effect of the overall face perception ability of the participants. Within the individually defined face-selective FFA, OFA, and object-selective LOC we selected a single voxel with the largest absolute beta difference in the intact versus noisy faces contrasts and used the signed difference to characterize the magnitude of the noise effect in these regions for each participant (for ROI definition, see Materials and Methods, Fig. 2.4*A*, and Table 2.1). This ROI-based semipartial correlation analysis revealed that the magnitude of noise effect measured in the right FFA—as expressed by fMRI response reduction in the noisy relative to the control condition— negatively correlated with the behavioral accuracy in the case of noisy faces (Fig. 2.4*B*): the larger the effect of noise in the right FFA, the lower the identity discrimination performance for noisy faces ($r_{(20)} = -0.57$, $p = 0.005$, CI = [$-0.83\ -0.14$], number of outliers (NO) = 0). On the other hand, we found no such correlations in the left FFA and bilateral LOC (Fig. 2.4*B*; $r_{(18)} = -0.30$, $p = 0.183$, CI = [$-0.67\ 0.23$], NO = 0; $r_{(15)} = 0.39$, $p = 0.106$, CI = [$-0.03\ 0.71$], NO = 0; and $r_{(12)} = 0.04$, $p = 0.897$, CI = [$-0.49\ 0.42$], NO = 4 for left FFA, right and left LOC, respectively).
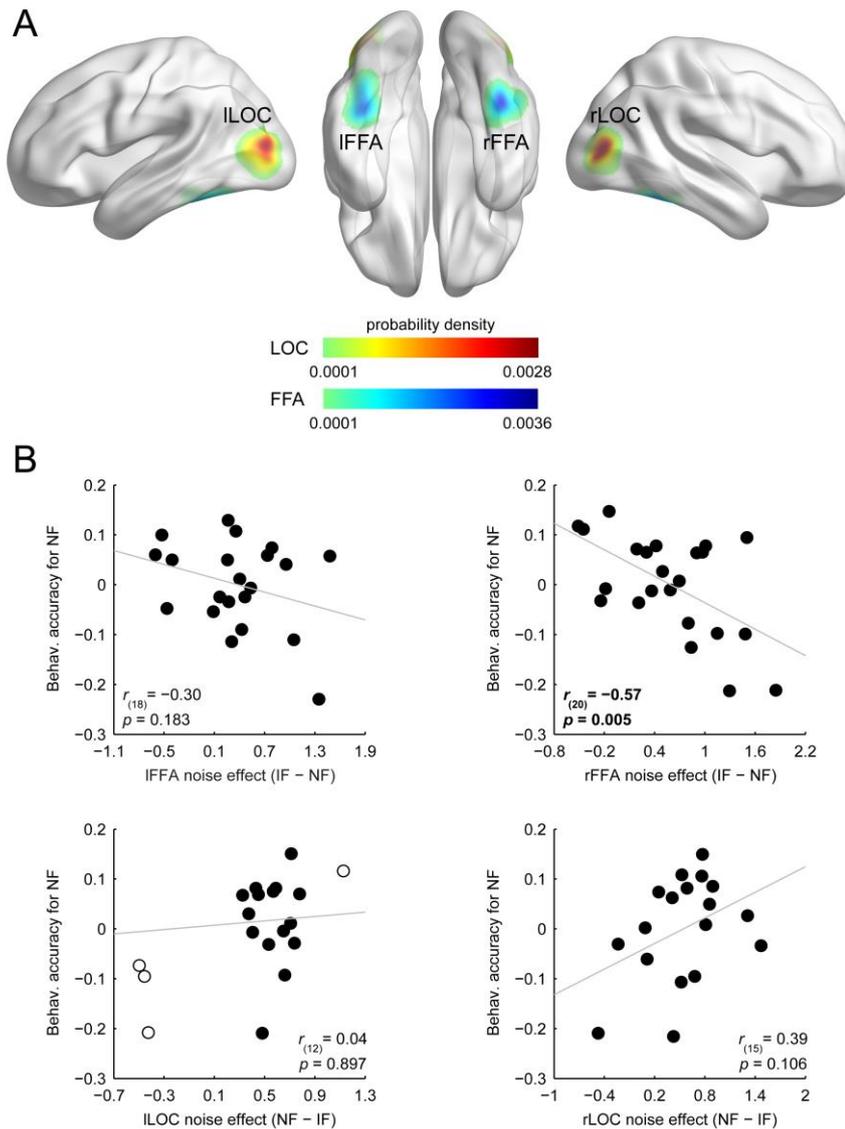
Figure 2.4. Results of the ROI-based correlation analysis. *A*, Probability density map illustrating the spatial distribution of the highest noise-effect voxels across participants in bilateral FFA and LOC. Color scales reflect probability density estimates (cool colors, FFA; warm colors, LOC). *B*, Relationship between the noise-induced modulation of the fMRI responses and the behavioral accuracy in discriminating noisy faces: smaller decrease of the fMRI responses in the right FFA indicated better identity discrimination. Due to the semipartial correlation procedure (see Materials and Methods, Correlation analysis), correlation scatter plots depict residual values on the *y*-axis. The *y*-axis values denote behavioral accuracy for noisy faces indexed by the residual correct response ratio. The *x*-axis values denote noise effect on the fMRI responses indexed by the beta difference in the IF versus NF contrast. Circles represent individual participants and bivariate outliers are marked with open circles. Diagonal line indicates linear least-squares fit. IF, intact faces; NF, noisy faces.

Note, we also failed to find significant correlation between the identity discrimination performance for noisy faces and the noise-induced fMRI response modulation in the OFA

($r_{(13)}$ = −0.36, p = 0.176, CI = [−0.77 0.23], NO = 0), a region in the inferior occipital gyrus, that was shown to be involved in an earlier feature-level processing stage of facial identity computations (for reviews, see [22, 124]). This appears to be in agreement with the results of our whole-brain random-effects analysis showing that fMRI responses in this region are not significantly different from each other for intact and noisy face stimuli. These results indicate that identity discrimination in the case of noisy faces could be associated primarily with right FFA processes.

2.4.4   Results of the intrinsic functional connectivity analysis

We investigated the behavioral relevance of the functional interactions between the voxels of the FFA and LOC exhibiting the highest noise effect by examining interindividual differences in resting-state functional connectivity in relation to the observed differences in identity discrimination accuracy for noisy faces. We first tested the extent to which BOLD responses in these regions were functionally correlated at rest. Reliable connectivity strengths were found between all ROI pairs using one-sample t tests ($t > 2.86$, $p < 0.01$ for all possible ROI pairs) (see Fig. 2.5*A*). The partial correlation analysis, used to control for the influence of the overall face perception ability of the participants on rsFC strength and noisy face performance, revealed that the functional connectivity strength between bilateral FFA and bilateral LOC correlated positively with the behavioral accuracy for noisy faces (Fig. 2.5*B*): the stronger the functional connectivity between these regions during rest, the better the face identity discrimination performance in the noisy condition (rFFA–rLOC: $r_{(12)}$ = 0.59, p = 0.020, CI = [0.21 0.88], NO = 2; rFFA–lLOC: $r_{(13)}$ = 0.65, p = 0.007, CI = [0.35 0.86], NO = 2; lFFA–rLOC: $r_{(11)}$ = 0.69, p = 0.006, CI = [0.51 0.91], NO = 2; and lFFA–lLOC: $r_{(13)}$ = 0.68, p = 0.004, CI = [0.42 0.87], NO = 1). Performance for noisy faces also correlated positively with the connectivity strength between the right and left FFA ($r_{(17)}$ = 0.59, p = 0.006, CI = [0.17 0.92], NO = 1). On the other hand, similar relationship was not detectable in the case of the right and left LOC ($r_{(14)}$ = −0.05, p = 0.841, CI = [−0.53 0.48], NO = 0).
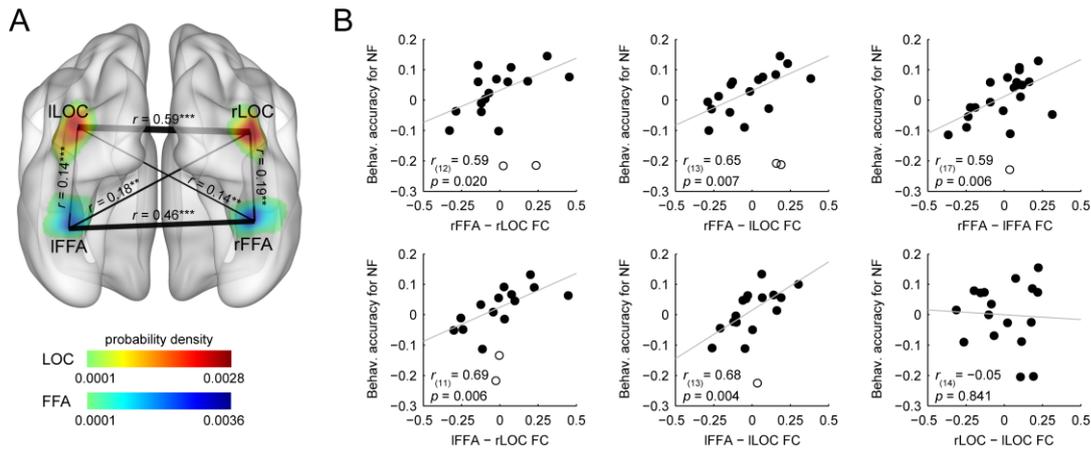
Figure 2.5. Results of the intrinsic functional connectivity analysis. *A*, Connections between the pairs of ROIs displayed as edges and overlaid on the probability density map from Figure 2.4*A*. The thickness of an edge represents the strength of the connection (correlation coefficients (*r*) averaged across subjects); significant correlations were found between all ROI pairs investigated. *B*, Scatter plots indicating the relationship between the intrinsic functional connectivity and the behavioral accuracy for noisy faces. The strength of the functional connectivity between bilateral FFA and LOC, as well as between the right and left FFA, correlated positively with the identity discrimination performance in the case of noisy faces. Due to the partial correlation procedure (see Materials and Methods, Correlation analysis), correlation scatter plots depict residual values on both axes. The *y*-axis values denote the behavioral accuracy for noisy faces indexed by the residual correct response ratio. The *x*-axis values denote the connection strength between a ROI pair indexed by the residual correlation coefficient. Circles represent individual participants and bivariate outliers are marked with open circles. Diagonal line indicates linear least-squares fit. NF, noisy faces; FC, functional connectivity (**$p < 0.01$, ***$p < 0.001$).

Since previous research has shown that resting-state functional connectivity between the FFA and OFA is associated with identity perception in the case of intact faces [99], we also tested the relation between the strength of the FFA–OFA intrinsic functional connectivity and identity discrimination performance for noisy faces. Although in accordance with previous results [42, 99, 103] we found a pronounced resting-state connectivity between the FFA and OFA ($t_{(15)} = 6.27$, $p < 0.001$ and $t_{(13)} = 4.57$, $p < 0.001$ for rFFA–rOFA and lFFA–rOFA, respectively), its strength was not correlated with the noisy face identification performance ($r_{(13)} = -0.16$, $p = 0.566$, CI = [−0.63 0.59], NO = 0 and $r_{(10)} = 0.28$, $p = 0.350$, CI = [−0.24 0.70], NO = 1 for rFFA–rOFA and lFFA–rOFA, respectively). In sum, these results suggest that face identity perception in the case of noisy faces is based on functional interactions between bilateral FFA and LOC.

2.5 Discussion

We have found that adding phase noise to face images leads to reduced and increased fMRI responses to faces in bilateral mid-fusiform gyrus and bilateral lateral occipital cortex, respectively, which is in agreement with previous results [62, 120]. Importantly, our results provide the first evidence that only in the right face-selective FFA did noise-induced modulation of the fMRI responses show a close association with the individual differences in face identity discrimination performance of noisy faces: smaller decrease of the fMRI responses was associated with better identity discrimination. This implies that the perception of noisy face images is based on the neural representations extracted from the right FFA. The robust behavioral face inversion effect also in the case of noisy images provides further support for the role of FFA in noisy face perception. Furthermore, our results also revealed that the strength of intrinsic functional connectivity within the visual cortical network composed of bilateral FFA and bilateral object-selective LOC predicts the participants' ability to discriminate the identity of noisy face images.

Right FFA subserves noisy face perception. Our results are in agreement with previous findings showing that representations extracted by the FFA embody the primary neural substrate of facial identity perception in the case of intact faces. It was found that fMRI responses in the FFA are closely associated with successful identification of faces but not non-face objects [37], as well as with the well-known marker of face-specific processing, the behavioral face inversion effect [40]. Based on its coordinates, the FFA subregion whose fMRI responses were associated with noisy face identity discrimination in our study appears to be in close correspondence with the face-selective region related to intact face perception in the mid-fusiform gyrus [37, 39, 40]. This anterior part of the FFA, referred to as mFus-faces [29] (for review, see [123]), shows greater fMRI adaptation to repeated face images than the more posterior pFus-faces [125], suggesting its pivotal role in identity perception. Given the suggested role of FFA in the behavioral inversion effect for intact faces (FIE, [18]) [40] we reasoned that if FFA also subserves noisy face perception, face inversion will impair behavioral responses in the case of noisy face stimuli as well. The robust FIE also in the case of noisy images indicates that similarly to intact faces, noisy ones are discriminated based on face-specific processes linked to FFA.

It is important to note that previous results concerning the role of FFA in identity perception in the case of faces with deteriorated facial information were ambiguous. On the one hand, it has been shown that scrambling or adding noise to face images leads to reduced fMRI responses in the FFA [119–121, 126], which is in accord with a large body of neuroimaging results

showing that the presence of noise in images strongly attenuates feature/object-selective visual cortical responses in the downstream, higher-level object-processing areas [126–130]. Based on these findings, facial feature processing in the FFA was expected to be impaired in the presence of noise. On the other hand, involvement of the FFA in the processing of noisy faces is implicated by the results of a recent study, in which no response reduction was found in the FFA as a result of adding phase noise to the face images [62]. Furthermore, it has also been shown that face-sensitive responses emerge first in the FFA when participants perform a face detection task in a paradigm where scenes containing faces are revealed gradually from visual noise [57]. Considering the difference in task conditions between these studies might help to reconcile the apparent discrepancies in the obtained results. In studies where fMRI responses in the FFA were found to decrease as a result of noise, data were acquired during either passive viewing or under task conditions where fine facial information was irrelevant [119–121]. Whereas, in the Bankó et al. study [62], where noise effects were absent in the FFA, participants performed a highly demanding face gender categorization task. As visual attention and task demands strongly affect fMRI responses in the FFA [121, 131–134], it is reasonable to assume that the enhancing effects of top-down attention in the Bankó et al. study [62] could have masked the noise-induced reduction of the FFA responses. This interpretation is in accordance with the results of a previous study [135] showing that decreasing motion coherence (i.e. making the stimulus noisier) leads to decreased MT+ responses only when the motion stimulus is task-irrelevant/unattended. In contrast, when motion is attended the effect of decreasing motion coherence disappeared or even reversed, leading to larger MT+ responses. Our present results are also in line with this account as using noisy face stimuli we obtained noise-induced reduction of the fMRI responses in the FFA under moderately demanding task conditions.

Occipitotemporal network underlies noisy face perception. Our findings also shed light on the visual cortical network that enables the extraction of identity information when stimuli are noisy, i.e. with deteriorated facial information. Previous research has shown that adding phase noise to the stimuli leads to increased fMRI responses in a region of bilateral LOC [62], whose coordinates closely correspond to the shape-selective, retinotopically organized LO2 area, which represents shape information within a spatial coordinate system [64, 104]. Based on these findings, we hypothesized that increased processing demands due to the distorted spatial localization of the facial features in the case of phase-randomized face images might trigger re-entrant processing mechanisms involving the LOC. Our intrinsic functional connectivity analysis provides the first direct evidence that this might indeed be the case, showing that the strength of the functional connectivity between bilateral LOC and FFA predicts the participants' ability to discriminate the identity of noisy face images. Although LOC is

considered primarily as an object-selective area [136–138], it shows elevated activation for faces as well, especially for inverted ones [40, 79, 139]. There is also evidence showing that the LOC is essentially involved in the feature-based processing of face images [126, 140–143] and its activation might contribute to better behavioral performance in face perception [143]. These findings provide support for our results showing that LOC processes are engaged in the extraction of face identity information for stimuli with deteriorated facial information.

Our resting-state connectivity analysis also revealed that functional connectivity between the left and right FFA was also closely associated with the identity discrimination performance for faces embedded in noise. This is in agreement with the results of numerous previous studies showing that despite the right hemisphere dominance for face perception [24, 30, 144, 145], interhemispheric interactions appear to be necessary for successful face recognition. The strong task-related [44, 146], background [43], and resting-state [42] functional connectivity between corresponding face regions in the two hemispheres (including the right and left FFA) suggests that face processing involves a bilateral network. Furthermore, it was also shown that bilateral presentation of face stimuli leads to improved performance compared with unilateral presentation [147–150]. Thus, there is converging evidence that left FFA mechanisms, mainly associated with featural processing [151–154], could facilitate face recognition in the right FFA through reciprocal connections especially when faces are disrupted in their structural content, as was the case in our study.

More generally, the results of our functional connectivity analysis provide further support that measuring resting-state connectivity is a useful tool for investigating behaviorally relevant functional interaction between visual cortical areas [99, 102, 103]. It has recently been shown that the strength of the intrinsic functional connectivity within the occipitotemporal face network predicts perceptual ability to process faces depending on stimulus/task properties. For example, it was demonstrated that the connectivity of the FFA with the OFA [99] and with the perirhinal cortex [103] is closely related to the behavioral face inversion effect. Together with the present results, these findings suggest that processing of facial features takes place via coordinated interaction within the visual cortical face network, relying on synchronized spontaneous neural activity between face-processing regions.

To conclude, these results imply that perception of facial identity in the case of noisy face images is subserved by neural computations within the right FFA as well as a re-entrant processing loop involving bilateral FFA and LOC.

A question that remains to be explored concerns whether the neural mechanisms implicated in processing of face images degraded by phase noise are those that also deal with other types of visual noise. Reducing phase coherence using the weighted mean phase technique [107] disrupts the spatial locations of features, while it leaves lower-level statistics of the images such as global spatial frequency amplitude spectrum, luminance, and contrast unaffected. Thereby, phase noise primarily affects higher-level object-processing mechanisms for coding and integrating the structural information of the images, which is supported by our results. On the contrary, previous research suggests that white noise [155] or scrambling [129] affects the processing of visual stimuli already in the early visual cortical areas, including the primary visual cortex. Thus, to clarify the validity of our results for other types of visual noise, further studies using different types of noise within one experimental framework are needed.

3 The relationship between repetition suppression and face perception

3.1 Introduction

It has been shown that sensory information processing is highly affected by short-term prior perceptual experience. When a sensory stimulus is repeated, the evoked neural signal is invariably smaller than the one observed for its first presentation. This phenomenon is observed for many sensory modalities and for various stimuli using different methods. For example, the response of the visually sensitive neurons of the inferior temporal cortex (IT) of the macaque brain decreases when a stimulus is repeated [156–163], an effect termed repetition suppression (RS). Similarly, in functional magnetic resonance imaging (fMRI) experiments stimulus repetitions lead to the reduction of the blood oxygenation level-dependent (BOLD) signal when compared with non-repeating stimuli (for a review see [164]), a phenomenon called fMRI adaptation (fMRIa). Although a large number of studies tested the neural mechanisms of RS in the last decades, there are still several open questions regarding this phenomenon. While prior studies typically connected RS to local or entirely bottom-up mechanisms, such as fatigue, sharpening, or response facilitation (for a review see [165]), recent studies emphasized the role of top-down factors, such as predictions and expectations [75]. Although current single-cell recording results suggest that a simple fatigue-related adaptation of the firing rate is, indeed, unable to explain RS related phenomena [166], the role of top-down effects is currently under heavy debate (for reviews see [74, 167, 168]). The few available human neurochemical studies suggest the role of gamma-aminobutyric-acid and acetylcholine in modulating neural responses during stimulus repetitions (for a review see [169]).

The behavioral relevance of the neural RS remains an interesting and open question. RS is generally believed to reflect short-term plastic processes of the neurons, as they adapt to the temporal context of the current environment. Thereby, RS reflects the flexibility of the neural system and its ability to adjust to continuously changing requirements, optimizing the performance of the individual [76]. However, so far we have only limited evidence of the direct relationship between RS and behavioral performance changes [170]. Previously, a long tradition of research connected RS to behavioral priming effects. Priming [171] is a phenomenon when the prior presentation of a related or identical stimulus leads to faster and more accurate responses for the target. Indeed, recent neuroimaging studies found that trials

leading to behavioral priming also lead to fMRIa in the fusiform and occipital face areas (FFA and OFA) of the human brain [82]. Similarly, repetition priming has also been related to fMRIa in several cortical areas for objects and scenes, including prefrontal, parietal, and occipitotemporal ones [80, 81]. However, a clear causal relationship could not been determined between behavioral priming and RS as of today. In fact, recent studies have raised doubts about the relationship of RS and priming: RS was either not specific to the "primed" conditions [172], or the magnitude of RS did not correlate with the amount of behaviorally observed priming effects [77]. These results suggest that RS and priming might co-occur but they are not necessarily connected to each other functionally.

A more direct approach for investigating the behavioral relevance of RS would be to test whether the individual fMRIa effect is related to the face perception ability of the participants. Gilaie-Dotan et al. [79] found that the fMRI responses in the FFA to repeated face presentations varying in identity similarity were associated with the perceived face similarity. Indeed, in patients of acquired prosopagnosia (an inability to recognize faces) due to the lesion of OFA, a lack of RS has been found in the FFA [59, 173], suggesting its functional relevance. Furthermore, another study, measuring intracerebral EEG, found strong RS for face identity in the right OFA on an electrode, whose stimulation disrupted behavioral face discrimination [174]. To test this relationship more directly, in the current study we investigated the association of fMRIa with the perceptual sensitivity of the participants for face stimuli in an identity discrimination task. We reasoned that if RS (and the consequent fMRIa) indeed reflects the better responding capacity of the neural system then this should manifest on the perceptual level as well. For this end, we compared the magnitude of fMRIa within areas of the core face-network as well as the extrastriate body area (EBA, [175]) as a control area, with the behavioral performance of the participants in a face identity discrimination task.

3.2 Materials and methods

3.2.1 Subjects

Altogether 30 Caucasian subjects (8 male; 2 left-handed; mean age ($\pm$ SD): 22.8 (3.2) years) participated in the experiment and gave informed written consent in accordance with the protocols approved by the Ethical Committee of the Friedrich Schiller University Jena. One subject had to be excluded from the study due to technical difficulties in the data acquisition. Therefore, the present results are based on the data of 29 subjects. None of them had any

history of neurological or psychiatric diseases, and all had normal or corrected-to-normal visual acuity.

3.2.2 Psychophysics experiment

To determine the face perception ability of the participants, they performed a three-alternative forced choice perceptual face identity discrimination task outside the scanner (Fig. 3.1).

Stimuli. In the psychophysics experiment, trials consisted of triplets of morphed faces. Front-view grayscale images of Caucasian male faces with neutral expression were cropped to eliminate external features and were equated for luminance and contrast. Triplets (Fig. 3.1) were obtained by first pairing two individuals and creating a linear morph continuum using a warping algorithm (JPsychoMorph, [106]). Altogether 78 continua were created from 13 individuals. Triplet members were selected from these continua as follows: face A and C were chosen to be the 20/80% and 80/20% points of the morph-space, respectively, while face B was taken from in between, such that the morph distance between the oddball image (e.g. C) and its neighbor (B) was larger than the distance between the other two images (e.g. A and B). This distance was based on pilot measurements to keep performance within the 60-70% range. Faces were presented upright and upside-down.
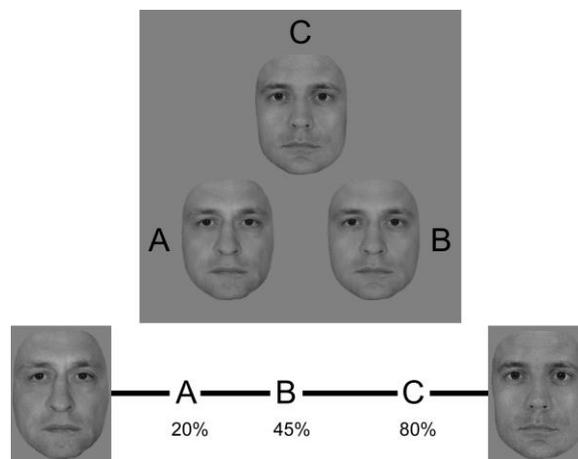
Figure 3.1. Example stimulus of the behavioral task performed outside the MRI scanner. By morphing two paired individuals (illustrated on the bottom), we created face triplets (top) including faces at 20/80% (A), 45/55% (B) and 80/20% (C) points of the morph-space and presented in a regular triangular arrangement upright and upside down (inverted). Please note that the letters are only for illustration purposes and were not presented in the actual experiments.

Triplets were displayed at the center of the screen on a uniform gray background in a regular triangular arrangement with 4° of visual angle eccentricity. Triplets measured ~11° × 12°, faces subtending 4.5° × 6.0° each, and were presented on a CRT display at a refresh rate of 60 Hz viewed from 85 cm. Stimulus presentation was controlled by MATLAB R2010a (The MathWorks Inc., Natick, MA, USA) using the Psychophysics Toolbox Version 3 (PTB-3) [108, 109] (http://psychtoolbox.org/).

Experimental procedure. Participants performed a three-alternative forced choice identity discrimination task. Subjects were required to select the face that differed the most from the other two (i.e. the oddball face). Each trial began with a cue (1°) appearing just above fixation for 100 ms, indicating the orientation of the upcoming stimuli (upright or inverted). Triplets were presented without a fixation dot under free-viewing conditions until subjects responded; trials were terminated after 5000 ms if no response had been made. Trials were separated by an inter-trial interval, which varied randomly between 900 and 1100 ms, with only the fixation dot present. Oddball faces appeared with equal probability in each of the three possible spatial positions. Each unique face triplet was presented only once per condition, randomly assigned to one of the three runs for each participant. Within a single run, the two conditions (upright/inverted) were intermixed and presented in random order. Each participant completed three runs, yielding 78 trials altogether for each condition.

3.2.3 fMRI experiment

The fMRI data analyzed in the current study was a subset of what we previously used to examine the face processing stages at which repetition probability affects fMRI adaptation [6]. However, here we aimed at investigating the functional relevance of repetition suppression in face processing. Therefore, we only analyzed data from blocks with high stimulus repetition probabilities where the repetition suppression effect was clearly evident and the largest.

Stimulation and Procedure. The experimental design—as also described in Grotheer et al. [6]—was similar to that of Summerfield et al. [75] and to that of Kovács et al. [176]. Briefly, 240 grayscale, digital photos of full-frontal Caucasian faces, similar to the face stimuli of Kovács et al. [176] and Kovács et al. [177], were fit behind a circular mask and either presented upright or inverted in different runs of fMRI recordings (Fig. 3.2*A*). No stimulus occurred in more than one trial during each run. Stimuli were placed in the center of the screen on a uniform gray background. A trial contained two faces presented subsequently for 250 ms each, separated by an inter-stimulus interval that varied between 400 and 600 ms and was followed randomly by a 1 or 2 s long inter-trial interval. The first stimulus (S1), was either

identical to (Repetition Trial, RepT) or different from the second stimulus (S2) (Alternation Trial, AltT). Stimuli subtended 2.75° of visual angle. To reduce local feature adaptation, the size of either S1 or S2 (chosen randomly) was reduced by 18%. The participants' task was to maintain central fixation throughout the trials and to signal the occurrence of target stimuli, which were reduced in size by 54%, via a speeded button push.

Stimuli were back-projected via an LCD video projector (NEC GT 1150, NEC Deutschland GmbH, Ismaning, Germany, with modified lens for short focal point) onto a translucent circular screen, placed inside the scanner bore. Presentation was controlled via MATLAB R2013a (The MathWorks Inc., Natick, MA, USA), using Psychophysics Toolbox Version 3 (PTB-3) [108, 109] (http://psychtoolbox.org/).

The two different trial types (AltT and RepT) were presented in two different types of blocks with varying repetition probabilities [6] (Fig. 3.2*B*; identical to the paradigm of Summerfield et al. [75]) in a run.
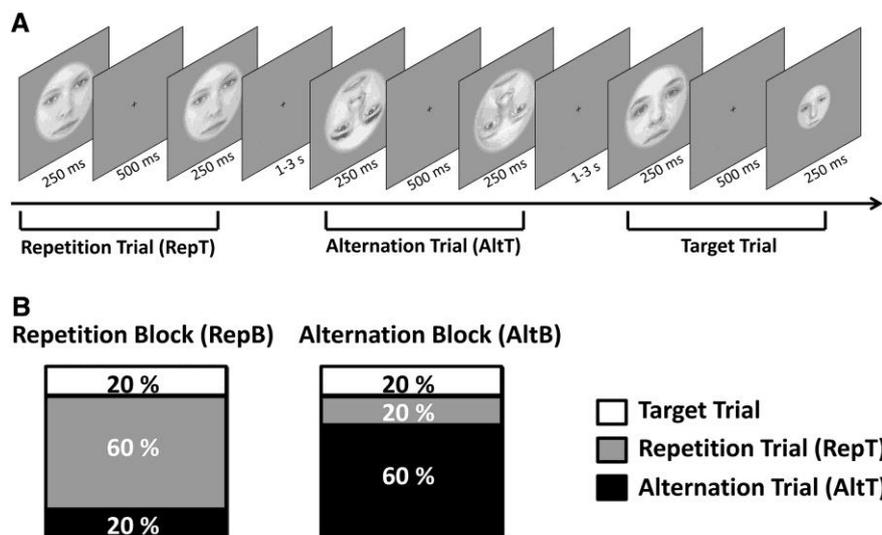
Figure 3.2. *A*, Stimulation parameters and arrangements. An upright repetition trial (RepT), an inverted alternation (AltT) and an upright target trial are illustrated. Please note that the upright and inverted trials were presented in different runs. *B*, The composition of the repetition and alternation blocks. During a run, RepBs and AltBs were each repeated four times. (Taken from [6].)

In the Repetition Blocks (RepB), 75% of the non-target trials were RepT while 25% were AltT (12 RepTs vs. 4 AltTs). In the Alternation Blocks (AltB), 75% of non-target trials were AltT and 25% were RepT (12 AltTs vs. 4 RepTs). With the exception of the first four trials, which were always drawn from the more frequent trial type of that specific block (RepT in RepB and AltT in AltB), RepT and AltT were presented randomly within the blocks. In addition, 20% of

The relationship between repetition suppression and face perception

all trials were target trials, whereas target trials could be AltT or RepT with the same relative probability. As we did not observe reliable fMRIa within the alternating blocks (see Fig. 3*B* of Grotheer et al. [6]), please note that in the current study, we only analyze the blocks where stimulus repetitions had high probabilities.

Both Alternation and Repetition Blocks contained 20 trials and were repeated 4 times during each run, so that a run contained 160 trials. The different blocks were separated from each other by a 7 s pause during which the phrase "*Short Break*" was presented centrally together with a countdown. Four runs were presented in total, whereas the order of upright and upside-down runs was counterbalanced across subjects.

3.2.4 fMRI scanning

Data were collected at the Friedrich Schiller University Jena (Jena, Germany) on a 3 Tesla Siemens Magnetom Trio scanner (Siemens Healthineers, Erlangen, Germany) equipped with a 20-channel head coil. During the functional blocks we continuously acquired images using a T2*-weighted GRE-EPI sequence (34 slices, 10° tilted relative to the subjects' axial plane determined by the AutoAlign protocol, TR =2000 ms; TE = 30 ms; in-plane resolution: 3x3 mm; slice thickness: 3 mm; 20 % inter-slice interval, FOV = 192 mm, acceleration factor = 2). To additionally obtain a 3D structural scan, high-resolution sagittal T1-weighted images were acquired using a 3D-MPRAGE sequence (TR = 2300 ms; TE = 3.03 ms; 1 mm isotropic voxel size, FOV = 256 mm).

3.2.5 fMRI data analysis

The analysis of the imaging data differs considerably from the one performed in our previous report [6]. Preprocessing and analysis of the imaging data were performed using the SPM12 toolbox (Wellcome Trust Centre for Neuroimaging, London, UK) as well as custom-made scripts running on MATLAB R2013b (The MathWorks Inc., Natick, MA, USA). The functional images were spatially realigned to the first EPI image within a session for motion correction. The anatomical T1-weighted image was coregistered to the mean functional T2*-weighted image generated during the realignment step followed by segmentation and normalization to the MNI-152 space using the new unified segmentation-normalization tool of SPM12. To spatially normalize functional images to MNI space we applied the deformation field parameters that were obtained during the normalization of the anatomical T1-weighted image. After the normalization procedure, functional images were spatially smoothed with an 8 mm full width at half maximum (FWHM) isotropic Gaussian kernel. The gray matter mask

derived from the segmentation of the anatomical image was used to restrict statistical analysis on the functional files. The 4 experimental conditions (AltB_AltT, AltB_RepT, RepB_AltT, RepB_RepT) as well as the target trials from our event-related sessions with upright and inverted faces were defined as separate regressors, which were convolved with the canonical hemodynamic response function (HRF) of SPM12, for a General Linear Model (GLM) analysis of the data. Movement-related variance was accounted for by the spatial parameters resulting from the motion correction procedure. A high-pass filter with a cycle-cutoff of 128 s was also implemented in the design to remove low-frequency signals. The prepared regressors were then fitted to the observed functional time series within the cortical areas defined by the gray matter mask. In order to specifically address the questions that we aimed to investigate in the current study, we used parameter estimates (i.e. beta weights) only for the RepB_AltT and RepB_RepT conditions. To obtain beta weights for AltT and RepT in RepB with equal number of trials, we used a bootstrap procedure (resampling without replacement, n = 1000) where for RepT 4 non-target trials were randomly chosen from each of the 4 RepBs yielding 16 RepTs per run, which was treated as a separate regressor in the GLM approach. This procedure was repeated 1000 times and the resulting 1000 beta weights were averaged for each condition and subject for further analysis (Fig. 3.3).
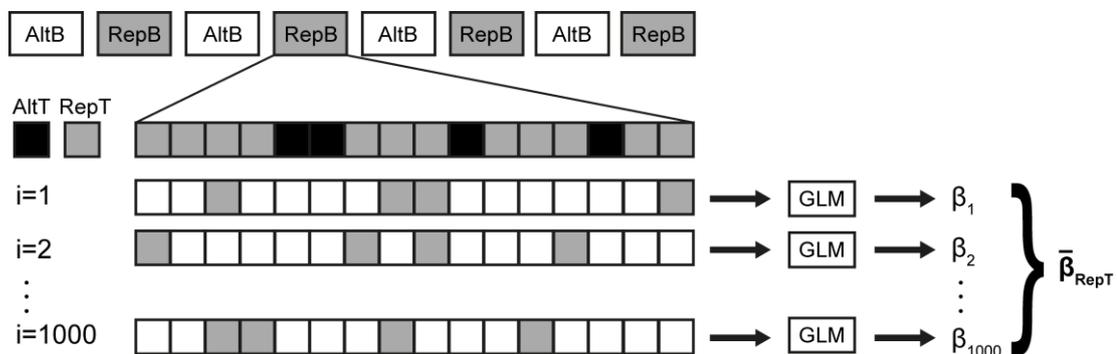
Figure 3.3. Bootstrap procedure. During the GLM analysis of the fMRI data, we applied a bootstrap procedure to estimate beta weights (β) based on equal number of trials for AltT (black) and RepT (gray) in RepB. For each bootstrap sample (i), we randomly selected 4 non-target RepTs from each of the 4 RepBs yielding 16 RepTs per run which constituted a separate regressor in the GLM approach. This procedure was repeated 1000 times and the resulting 1000 beta weights were averaged for each condition and subject for further analysis. Please note that in this figure only the non-target trials in a single RepB are represented.

ROI definition. A separate functional localizer run (640 s long; 20 s epochs of faces, objects, human bodies, and Fourier randomized versions of faces [107], interleaved with 20 s of blank periods; 2 Hz stimulus repetition rate; 300 ms exposition time; 200 ms blank) was used to

determine regions of interest (ROIs) for each participant. The fusiform face area (FFA) in the mid-fusiform gyrus was identified as an area responding more strongly to faces than objects and Fourier randomized versions of faces. The occipital face area (OFA) in the inferior occipital gyrus was determined as an area showing significantly stronger activation to faces than Fourier randomized versions of faces, while the extrastriate body area (EBA) localized in the lateral occipital cortex was determined as an area responding more intensely to human bodies relative to objects. Peak voxel activity of all ROIs was required to meet a minimum threshold of $p_{\text{uncorrected}} = 0.001$. We only included subjects in the analysis for whom we could individually define these ROIs (for details, see Table 3.1).

ROI	x	y	z	N
rFFA	40 ± 0.7	-52 ± 1.4	-18 ± 0.6	27
lFFA	-39 ± 0.5	-54 ± 1.3	-20 ± 0.6	22
rOFA	42 ± 0.7	-77 ± 1.1	-10 ± 0.9	24
lOFA	-38 ± 0.6	-80 ± 1.1	-13 ± 0.7	24
rEBA	52 ± 0.7	-70 ± 0.9	7 ± 0.8	26
lEBA	-49 ± 0.8	-75 ± 1.1	8 ± 0.9	24

Table 3.1. Peak voxel coordinates for the regions of interest (ROIs). The MNI coordinates (x, y, z in millimeters) of the peak voxels in the case of FFA, OFA, and EBA are reported. Provided data are mean $\pm$ SEM across participants (N) for whom these regions were individually identifiable at the threshold of $p_{\text{uncorrected}} < 0.001$.

3.2.6 Statistical analysis

To determine the magnitude of fMRIa in these regions, mean beta weights for AltT and RepT in the Repetition Blocks were extracted from a 6 mm radius sphere around the peak voxel of each individually defined ROI, and entered into a two-way ANOVA with hemisphere (L vs. R) and trial (AltT vs. RepT) as within-subject factors. To examine whether fMRIa measured in the investigated ROIs is related to face-selective perceptual ability, we correlated the individual fMRIa magnitudes—calculated by subtracting beta weights of RepT from that of AltT—with subjects' performance on face identity discrimination. To control for the individual differences in low-level visual feature processing and overall object perception ability, we regressed out the fMRIa and identity discrimination performance for inverted faces from those for upright faces, respectively, before calculating correlations between these two measures. Subjects with behavioral face inversion effect (N = 4; calculated by subtracting performance for inverted faces from that for upright faces) below one standard deviation (SD

= 0.105) from the group mean (mean = 0.084) were excluded from this correlation analysis. These subjects had higher performance for inverted faces than upright faces, which suggests poor face-selective processing or insufficient task engagement. Since the assumption of bivariate normality was fulfilled for all correlation pairs investigated (HZ < 0.20, p > 0.372, [178]), skipped Pearson's correlation coefficients were calculated with the Robust Correlation Toolbox [118] in MATLAB. Bivariate outliers were detected using an adjusted box-plot rule and removed in the computation of skipped correlations. For correlation coefficients (r), 95% confidence intervals (CI) were calculated based on 1000 samples with the percentile bootstrap method implemented in the toolbox. Correlation strengths were compared with the test proposed by Zou [179]. Using this method two-sided 95% CIs were constructed for a difference between two dependent overlapping correlations based on their bootstrapped CI-s derived from the robust correlation analysis. Participants with missing data from any of the variables of interest were excluded for a given analysis.

3.3 Results

3.3.1 Behavioral results

Participants performed the three-alternative forced-choice identity-discrimination task with $61.5 \pm 1.8\%$ (mean percent correct ± SEM) accuracy and showed a robust face inversion effect (FIE, [18]), i.e. significantly higher performance for upright as compared to inverted faces ($t_{(28)} = 4.32$, $p < 0.001$). When testing for the correlation between individual differences in face-selective perceptual ability and fMRIa, performance for inverted faces was used as a covariate to control for the individual differences in overall visual object perception.

3.3.2 fMRI adaptation

Fig. 3.4 presents the average BOLD signal separately for AltT and RepT in the case of upright (Fig. 3.4*A*) and inverted faces (Fig. 3.4*B*).
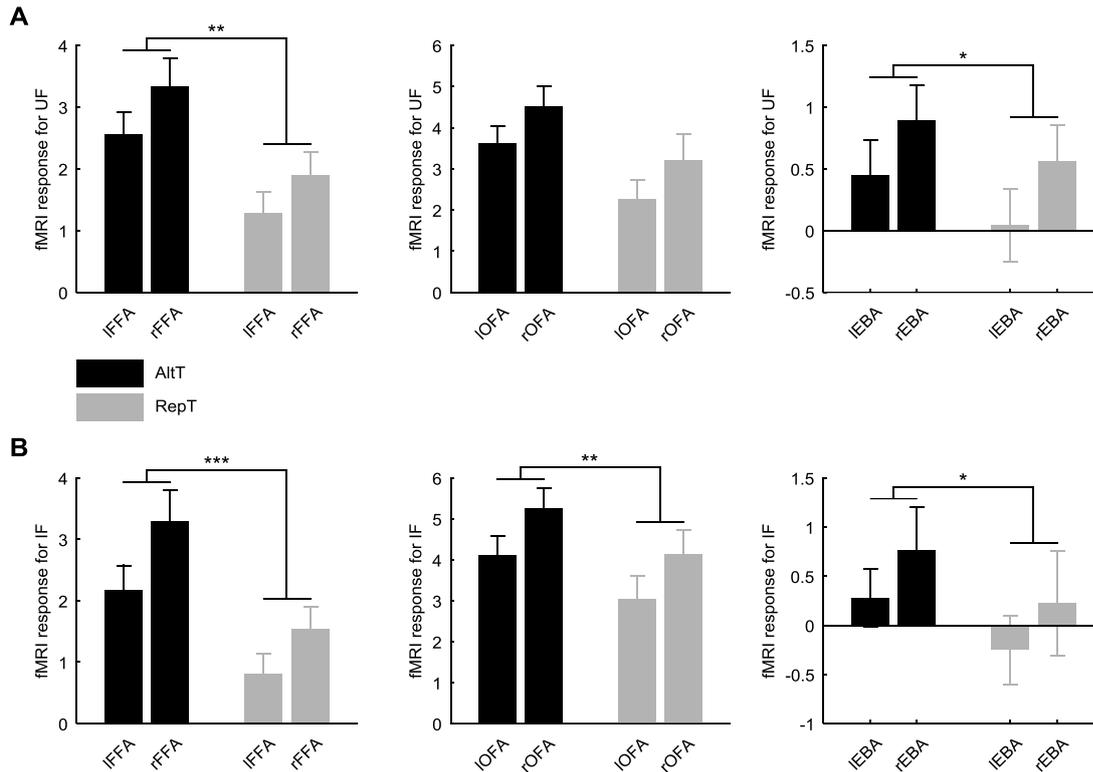
Figure 3.4. Average activation (± SEM) profiles for the left and right FFA (left), OFA (middle), and EBA (right) when faces were presented upright (A) and inverted (B). We found fMRIa, i.e. reduced fMRI responses for repeated (RepT) as compared to alternating faces (AltT) for all ROIs investigated in the case of both upright and inverted conditions. Black bars represent AltT; gray bars represent RepT. UF, upright faces; IF, inverted faces ($*p < 0.05$, $**p < 0.01$, $***p < 0.001$).

In agreement with previous results [70, 75, 176, 180–182], we found significant fMRIa, i.e. reduced BOLD signal for repeated (RepT) as compared to alternating faces (AltT) in the FFA and a moderate fMRIa in the OFA for upright faces (main effect of trial type for upright faces: $F_{(1,21)} = 8.25$, $p = 0.009$ and $F_{(1,21)} = 3.10$, $p = 0.093$ for the FFA and OFA, respectively) and also significant fMRIa in these regions for inverted faces (main effect of trial type for inverted faces: $F_{(1,21)} = 22.54$, $p < 0.001$ and $F_{(1,21)} = 9.89$, $p = 0.005$ for the FFA and OFA, respectively), as we reported in our previous work [6]. In addition, fMRI responses in the right hemisphere were more pronounced compared to the left hemisphere for each condition in the case of both upright (main effect of hemisphere for upright faces: $F_{(1,21)} = 15.81$, $p = 0.001$ and $F_{(1,21)} = 13.35$, $p = 0.002$ for the FFA and OFA, respectively) and inverted faces (main effect of hemisphere for inverted faces: $F_{(1,21)} = 18.03$, $p < 0.001$ and $F_{(1,21)} = 5.35$, $p = 0.031$ for the FFA and OFA, respectively) indicating the right hemisphere dominance in face processing [24, 30, 145, 183–185]. We also measured fMRIa in a region outside the typical face-processing network, specifically in the extrastriate body area (EBA) which served as a control region. The EBA showed a significant BOLD response reduction in the case of RepT relative

to AltT for upright (main effect of trial type for upright faces: $F_{(1,23)} = 4.56$, $p = 0.044$) and inverted faces (main effect of trial type for inverted faces: $F_{(1,23)} = 5.61$, $p = 0.030$) as well. The interaction of trial type and hemisphere was not significant for any of the tested areas in the case of both upright ($F < 1.08$, $p > 0.310$ for all comparisons) and inverted faces ($F < 1.88$, $p > 0.190$ for all comparisons). When testing for the correlation between individual differences in the magnitude of face-specific fMRIa and perceptual ability, fMRIa for inverted faces was used as a covariate to control for individual differences in the magnitude of the low-level feature adaptation effect.

3.3.3 Correlation of face discrimination accuracy and fMRIa

First, we calculated the magnitude of fMRIa by subtracting the BOLD response during RepT from that of AltT for each subject and area separately. Since we found a strong positive correlation between the fMRIa of the left and right hemisphere homologues of each tested area ($r_{(18)} = 0.75$, $p < 0.001$, CI = [0.35 0.94], number of outliers (NO) = 2; $r_{(19)} = 0.90$, $p < 0.001$, CI = [0.80 0.96], NO = 1 and $r_{(21)} = 0.51$, $p = 0.012$, CI = [0.30 0.72], NO = 1 for the FFA, OFA, and EBA, respectively), we averaged fMRIa across hemispheres to test for its correlation with face discrimination accuracy. To control for the individual differences in low-level visual feature processing and overall object perception ability, we regressed out the fMRIa and identity discrimination performance for inverted faces from those for upright faces, respectively, before calculating correlations between these two measures. The Skipped Pearson correlation analysis revealed a strong positive correlation between fMRIa and identity discrimination performance in the FFA (Fig. 3.5*A*; $r_{(16)} = 0.72$, $p < 0.001$, CI = [0.41 0.91], NO = 0) and OFA (Fig. 3.5*B*; $r_{(18)} = 0.59$, $p = 0.006$, CI = [0.32 0.83], NO = 0), but not in the EBA (Fig. 3.5*C*; $r_{(18)} = 0.17$, $p = 0.470$, CI = [−0.23 0.58], NO = 1). The magnitude of correlation for the FFA and OFA with behavior was not different (CI = [−0.30 0.35]) and significantly greater than that for the EBA (CI = [0.10 1.08] and CI = [0.09 1.02] for the FFA and OFA, respectively). These findings suggest that genuine face-selective perceptual ability is associated with the fMRIa only in the core face-processing areas.
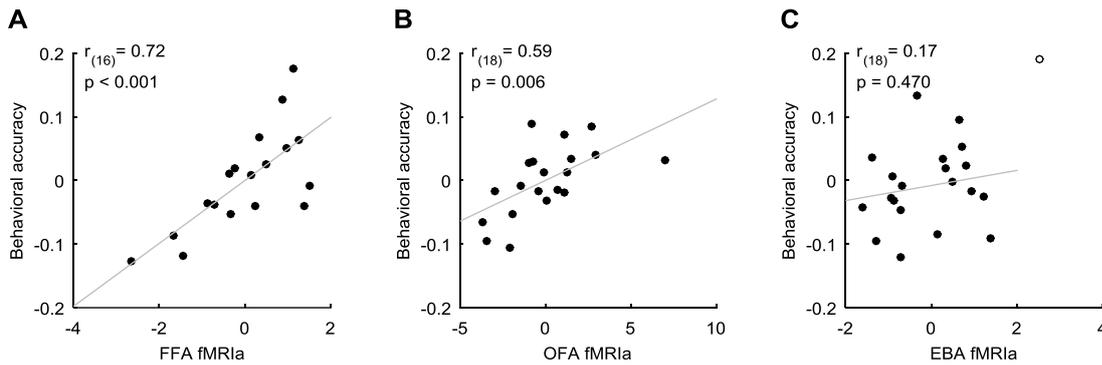
Figure 3.5. Correlation between behavioral accuracy and fMRIa for the FFA (*A*), OFA (*B*), and EBA (*C*). Significant correlation was found in the case of the FFA and OFA, but not for the EBA. Due to the regression-based approach (see Methods for details) correlation scatter plots depict residual values on both axes. *y*-axis values denote behavioral accuracy in the face identity discrimination task indexed by the residual correct response ratio. *x*-axis values denote the fMRIa indexed by the residual beta difference in the AltT vs. RepT contrast. Circles represent individual participants and bivariate outliers are marked with open circles. Diagonal line indicates linear least squares fit.

3.3.4 Correlation of fMRIa among the FFA, OFA, and EBA

To test whether fMRIa reflects common or different underlying mechanisms in the tested visual cortical areas, we calculated Skipped Pearson pairwise correlations of fMRIa magnitudes among the three regions after regressing out fMRIa for inverted faces. The results revealed that the magnitude of fMRIa in the FFA correlates positively and strongly with that of the OFA (Fig. 3.6*A*; $r_{(15)} = 0.81$, $p < 0.001$, CI = [0.59 0.94], NO = 0), but not with that of the EBA (Fig. 3.6*B*; $r_{(15)} = 0.05$, $p = 0.841$, CI = [−0.47 0.64], NO = 2). Furthermore, the strength of the correlation between FFA and OFA is significantly larger than between the FFA and EBA (CI = [0.18 0.97]). The fMRIa in the OFA showed a moderate, but significant correlation with that in the EBA (Fig. 3.6*C*; $r_{(16)} = 0.53$, $p = 0.025$, CI = [0.10 0.83], NO = 2), and the magnitude of this correlation did not differ significantly from that of the OFA and FFA (CI = [−0.15 0.59]). These findings imply that fMRIa might involve different components: one is mediated by neural mechanisms that are specific to the core face-processing network and another which affects the fMRI responses in the OFA and EBA, but not in FFA.
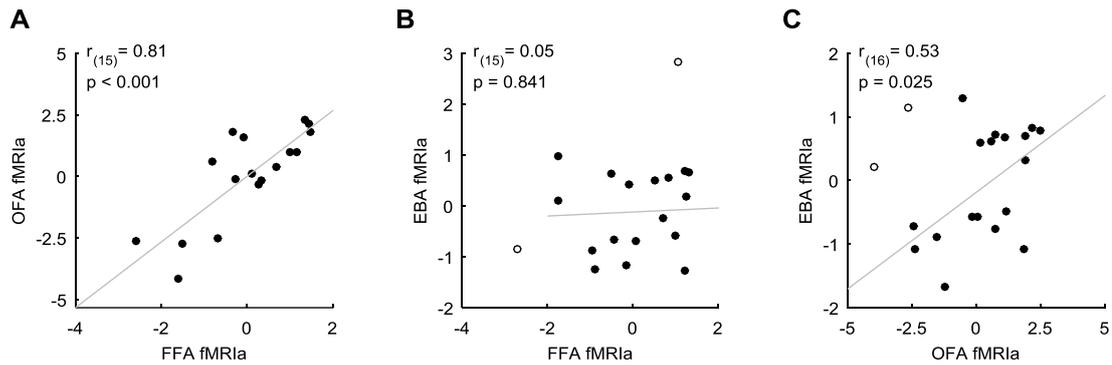
Figure 3.6. Correlation between fMRIa observed in the FFA and OFA (*A*), in the FFA and EBA (*B*) and in the OFA and EBA (*C*). Significant correlation was found between the magnitude of fMRIa measured in the FFA and OFA, as well as in the OFA and EBA, but not in the FFA and EBA. Due to the regression-based approach (see Methods for details), correlation scatter plots depict residual values on both axes. *y*- and *x*-axis values denote the fMRIa indexed by the residual beta difference in the AltT vs. RepT contrast. Circles represent individual participants and bivariate outliers are marked with open circles. Diagonal line indicates linear least squares fit.

3.4 Discussion

The major results of the current study can be summarized as follows: (1) The magnitude of fMRIa measured in the FFA and OFA, but not in the EBA, correlates positively with the behavioral performance of participants in a demanding face discrimination task. The higher the magnitude of the fMRIa for repeated faces, the better the face identity discrimination performance. (2) The observed fMRIa correlates between OFA and FFA, as well as between OFA and EBA, but not between FFA and EBA. These findings suggest that there is a face-selective repetition-induced fMRIa within the core face-processing network composed of the FFA and OFA, which reflects adaptive face processing mechanisms that are closely associated to face identity perception.

Network specific fMRIa. The fact that the observed fMRIa correlated between OFA and FFA, also between OFA and EBA, but not between FFA and EBA allows for multiple conclusions. First, it supports further the close connection between OFA and FFA [55]. Recent studies suggest that the OFA and FFA are closely and reciprocally connected to each other [43, 44, 186, 187] and the current results provide further functional evidence of this connection by showing that even the response reduction, signaling the sensitivity of neurons to repetitions, is related in the two areas. Our results are in agreement with previous findings from patients with acquired prosopagnosia showing that despite the preserved preferential activation for faces, adaptation effects for face identity in the right FFA are absent following lesions encompassing

the right OFA [59, 173]. This implies that fMRIa in the right FFA is the result of an intact re-entrant processing loop between these two regions. Furthermore, the close correlation of fMRIa in FFA and OFA supports the conclusion of Ewbank et al. [70]. These authors found that the repetition of a face having the same or different size affected the forward (OFA-to-FFA) and backward (FFA-to-OFA) connections specifically. Authors suggested that the fMRIa of a given region reflects the change of reciprocal (forward and backward) cross-region connectivity rather than merely the neural changes within that region. Second, the different correlation patterns we found between fMRIa in the OFA, FFA, and EBA imply that fMRIa might involve different components: one is mediated by neural mechanisms specific for the core face-processing network composed of the FFA and OFA and another which affects fMRI responses in the OFA and EBA, but not in FFA. This, in turn, also confirms previous results that suggest that the EBA is not part of the core face-processing cortical network [22].

The fact that we found a significant fMRIa in the EBA as well might be surprising for the first glance. Indeed, if an area shows adaptation after being exposed to its less- or non-preferred stimulus (i.e. a face for the body-part sensitive neurons) is surprising if one only considers response fatigue as the neural mechanisms of RS. Firing rate fatigue indeed predicts that the magnitude of adaptation essentially depends on the firing rate of that given neuron to the adapter stimulus. In other words, the larger the response for the adapter, the larger RS one should observe. However, recent single-cell studies disagree with this logic. Liu et al. [188] reported that the magnitude of RS does not correlate with the trial-to-trial firing rate of a neuron. Moreover, Baene and Vogels [189] showed that the degree of RS can even be inversely related to the response magnitude, given for the adapter stimulus. Finally, Sawamura et al. [161] showed that RS can be different for two different adapter stimuli that otherwise elicit the same response magnitude in the neuron. Altogether, these results question the direct relationship between stimulus preference and the magnitude of elicited RS. Therefore, it is possible that face stimuli, which elicit a significant response in the EBA as well [190, 191], elicit fMRIa as well.

fMRIa is associated with discrimination performance. The relationship of occipitotemporal activity with behavioral performance in visual stimulus processing was extensively addressed in the past. The activity of FFA and/or OFA has been related to the detection, recognition, or discrimination of faces [1, 37, 192, 193]. Huang et al. [39] measured face recognition in an old/new paradigm and found that the participants' recognition ability correlated with the face selectivity of the FFA and OFA, measured by estimating the differential response of the areas for face and non-face object stimuli. However, a very recent study which directly addressed the relationship between face identity memory and face selectivity in the FFA, failed to find

correlation between these two measures, except when correlating performance for the most difficult trials including noisy images with the activity in the center region of the FFA [31]. This suggests that both the nature of the behavioral task (e.g. perceptual or memory) and task difficulty might affect whether an association between behavioral and neural measures will be observed. Furthermore, the way FFA face sensitivity is measured appears to be similarly important. The findings of Nasr and Tootell [194] support this conclusion. Authors measured the activity of FFA and of the anterior face patch at the anterior tip of the collateral sulcus and found that only the activity of the more anterior area correlated with response accuracy. Previous results indicate that measuring face sensitivity by fMRI adaptation might be more suitable to uncover relationship between FFA activity and face perception [195, 196].

So far only one study tried to correlate the repetition related signal reduction to behavioral performance. Furl et al. [38] tested developmental prosopagnosics and healthy controls and correlated their face identification ability with identity and facial expression specific fMRIa. Authors found neither clear group differences nor any correlation for fMRIa with face identification. Also, Avidan et al. [197] found normal fMRIa in the FFA and OFA in developmental prosopagnosics and suggested that the fMRIa in these regions is not sufficient for normal face perception ability. These results might seem to contradict those of the current study. However, the approach of the two studies is sufficiently different to explain the opposing results. While in the current study participants performed a demanding perceptual face discrimination task, Furl et al. [38] used an extensive test battery and PCA analysis to compute a factor score and used this score as a covariate in the regression analysis of the fMRI data. As the test battery contained several perceptual and memory-related tests, it is likely that their behavioral measure reflects more complex face encoding processes as compared to the task applied in the current study. Therefore, it is possible that the fMRIa of the occipitotemporal areas is associated more closely with perceptual than to higher-level, associative or memory-related functions. This, in turn, would explain the apparently discrepant results of the Furl et al. [38] and the current study. Avidan et al. [197], on the other hand, used blocks of 12 different or identical faces to elicit fMRIa. Therefore, it is possible that the resulting neural adaptation is less sensitive to interindividual differences than the fMRIa elicited by short presentations of pairs of stimuli in the current study.

We observed significant correlation of behavioral performance with fMRIa in both OFA and FFA. Traditional models of face perception [22, 124] assume a hierarchical model where information flow from early visual cortices towards the OFA is responsible for face detection and categorization and the FFA and the superior temporal sulcus (STS) represents a higher-level face encoding, where identification and processing of facial expressions occurs.

However, the simple feed-forward processing of faces is questioned by recent prosopagnosic [59, 173] and transcranial magnetic stimulation [198] studies. Altogether, these recent results support a more parallel, non-hierarchical model where OFA and FFA are strongly connected (for a recent review see [16]). The similar correlation of FFA and OFA with behavioral performance supports this conclusion.

The neural basis of RS is unclear as of today and this complicates its association to behavioral measures. It is nonetheless generally assumed that RS reflects the specific encoding of the repeated feature or stimulus. In the current study, we measured the fMRI correlate of neural RS for the repetition of the same images with a strong variation in size to reduce low-level image feature adaptation. Furthermore, we controlled for the individual differences in low-level visual feature processing and overall object perception ability by using a regression-based approach, which provides a more precise and fine-grained picture of the relationship between fMRI adaptation within the core face-processing network and genuine face-selective perceptual ability. Whether this relationship is merely correlational or causal will require further studies, possibly combining neuroimaging and brain-stimulation techniques. The causal nature of this relationship, however, is suggested by a recent study. Yang et al. [199] tested the same acquired prosopagnosic patient as Schiltz et al. [173] and Steeves et al. [59]. Their findings suggested that the right anterior temporal lobe contains image-invariant face representations (signaled by normal RS) that can persist despite the absence of RS in the right FFA and OFA, but this representation is not sufficient for normal face recognition.

It should be noted that for the current study we only used the data from the blocks with high repetition probabilities of Grotheer et al. [6] as fMRIa was only measurable within these blocks. One can argue that the observed RS is more related to the implicit capacity of the participants to detect the probability of repetitions than to face perception per se. The fact that in spite of this confound we did find a strong and significant relationship between behavioral performance and RS suggests that this confound is unable to interact with the strong correlation of RS and face discrimination performance. It can be reasoned that within the framework of predictive coding models of perception [67], a good generative model of faces can produce better predictions of subsequent stimulations, which leads to better performance and reduced concomitant prediction error unit activity, i.e. fMRIa. If one accepts this argument then the likelihood of finding a relationship between behavior and fMRIa is more likely in the repetition blocks, where the expectation of repetition reduces uncertainty and enhances predictions and therefore the magnitude of fMRIa [75], compared to blocks where such repetitions are surprising. Nonetheless, this should be taken into account in future studies which should elicit RS in blocks with different statistics as well.

In conclusion, the current study has explored the behavioral relevance of the well-known phenomenon of repetition suppression (RS) for face images. We found that the RS as measured with BOLD fMRI in the core face-processing areas, namely in the fusiform face area (FFA) and occipital face area (OFA) is closely associated and predicts individual differences in face perception ability suggesting functionally relevant repetition suppression processes involved in face perception.

4 Conclusions and possible applications

The findings of the above experiments provide the first evidence that the fusiform face area (FFA) plays an important role in identity perception even in the case of noisy faces or faces embedded in a temporal context. Information processing in the FFA seems to highly depend on the context in which faces occur and its efficiency predicts individual face perception ability. Our results also shed light on the visual cortical network underlying the adaptive recurrent neural processes that are recruited to support successful face processing even under these challenging conditions.

We found that adding phase noise to face images led to reduced and increased fMRI responses in the mid-fusiform gyrus and the lateral occipital cortex (LOC), respectively, which is in agreement with previous findings [62, 120]. Importantly, our results showed, for the first time, that the noise-induced modulation of the fMRI responses in the right face-selective FFA was closely associated with individual differences in the identity discrimination performance of noisy faces: smaller decrease of the fMRI responses was accompanied by better identity discrimination. This implies that the perception of noisy face images is based on the neural representations extracted from the right FFA. The robust behavioral face inversion effect previously associated with FFA processes [40] was also found in the case of noisy face images providing further support for this finding. Our results also shed light on the visual cortical network that enables the extraction of identity information when stimuli are noisy, i.e. with deteriorated facial information. Our intrinsic functional connectivity analysis provides the first direct evidence that the strength of the functional connectivity between the bilateral shape-selective LOC and FFA predicts the participants' ability to discriminate the identity of noisy face images. These results imply that perception of facial identity in the case of noisy face images is subserved by neural computations within the right FFA as well as a re-entrant processing loop involving bilateral FFA and LOC.

Our results also revealed the contribution of occipitotemporal short-term adaptation processes—mediating the effect of prior perceptual experience—to face identity perception. In agreement with previous results [70, 75, 176], we have found that repeating identical face images elicits a robust decline in fMRI responses (fMRI adaptation, i.e. fMRIa) of the core face-processing areas, namely the FFA and OFA. Furthermore, we have also found fMRIa in the extrastriate body area (EBA). Importantly, we extend these findings by providing the first evidence that the face-selective fMRIa within the core face-processing network composed of

the FFA and OFA is closely associated with individual differences in face identity perception ability: the higher the magnitude of the fMRIa for repeated faces, the better the face identity discrimination performance. Moreover, we found a strong correlation of the fMRIa between OFA and FFA and also between OFA and EBA, but not between FFA and EBA. These findings suggest that there is a face-selective component of the repetition-induced reduction of fMRI responses within the core face-processing network, which reflects functionally relevant adaptation processes involved in face identity perception. Our results corroborate previous experimental and modeling findings implying that fMRIa to faces is a consequence of interactions between occipitotemporal regions [70, 200] rather than being a localized effect such as neuronal fatigue per se, and also provide support for the behaviorally relevant predictive coding [65–68] in the visual system.

Taken together, our results provide important new insights into the adaptive information coding processes within the extensive visual cortical face-processing network, especially regarding the recurrent neural mechanisms that enable efficient and robust human face perception even under suboptimal viewing conditions.

Understanding the strategies that the visual system employs in natural unconstrained settings could be the first step translating them into machine-based face recognition algorithms (see [201] for a review). Recognizing faces embedded in environmental and/or sensor noise is one of the most important longstanding challenges in machine vision systems. The knowledge of the neural mechanisms behind the recognition of noisy faces can facilitate the development of more robust face recognition algorithms. An iterative feedback neural network structure could be proposed containing two base modules, one that is trained on images of clear faces, and one that is responsible for image denoising. The dynamic interaction between these modules could contribute to improved accuracy and efficiency as compared to current face recognition systems.

More generally, our results provide further support that using task-based and resting-state functional connectivity fMRI methods is a useful tool for exploring precise and fine-grained relationship between brain and behavior by showing that the massive interindividual variability observed in face perception and also in its neural correlates measured during task and rest conditions is closely and selectively associated. Thus, advancing the knowledge of neural mechanisms underlying face perception at both regional and network level is a key issue to develop training programs including fMRI-based neurofeedback techniques (fMRI-NF) (see [202, 203] for reviews). Recent advances in fMRI-NF techniques reveal that participants can modulate the neural properties of both their individual brain regions and

functional brain networks through real-time neurofeedback [204–208]. Using this method, participants could self-regulate the interactions between their face-processing regions, which could help to improve the efficacy of visual cortical processing of facial information, especially in prosopagnosia where these interactions seem to be impaired [209–211].

5 Summary

5.1 New scientific results

1. Thesis: I have shown that perception of facial identity in the case of noisy face images is subserved by neural computations within the right FFA as well as a re-entrant processing loop involving bilateral FFA and LOC.

Published in [1], [3].

Previous research has made significant progress in identifying the neural basis of the remarkably efficient and seemingly effortless face perception in humans. However, the neural processes that enable the extraction of facial information under challenging conditions when face images are noisy and deteriorated remains poorly understood. Here we investigated the neural processes underlying the extraction of identity information from noisy face images using fMRI. For each participant, we measured (1) face identity discrimination performance outside the scanner, (2) visual cortical fMRI responses for intact and phase-randomized face stimuli, and (3) intrinsic functional connectivity using resting-state fMRI.

1.1. I have shown that noisy face discrimination is also based on face-specific processes as opposed to discrimination based on low-level stimulus features.

Combined behavioral and neuroimaging results provided strong evidence for specialized face processing (for reviews see [16, 17]) linked to FFA mechanisms [37–39]. Yovel and Kanwisher [40] has revealed that the most reliable marker of face-specific processing, namely the behavioral face inversion effect (FIE, [18])—i.e. the significant drop in discrimination of upside-down (inverted) relative to upright faces—is closely associated with the fMRI response in the FFA. Therefore, we reasoned that if FFA is the primary neural substrate also for noisy face perception, face inversion would impair behavioral responses in the case of noisy face stimuli as well. We found robust face inversion effects (i.e. decreased accuracy for inverted faces) in the case of both intact and noisy face conditions, which did not differ significantly in magnitude (Fig. 2.2). These behavioral findings suggest that the neural mechanisms involved in the processing of noisy faces might be similar to those of faces without noise, presumably mediated by the FFA.

1.2. Based on whole-brain analysis, I found that the presence of noise led to reduced and increased fMRI responses in the mid-fusiform gyrus and the lateral occipital cortex, respectively. Furthermore, the noise-induced modulation of the fMRI responses in the right face-selective fusiform face area (FFA) was closely associated with individual differences in the identity discrimination performance of noisy faces: smaller decrease of the fMRI responses was accompanied by better identity discrimination.

It has been suggested [62, 63] that in the case of phase-randomized face images the increased processing demand due to the distorted spatial localization of the facial features might lead to the engagement of a re-entrant processing loop involving the FFA and a region of the lateral occipital cortex (LOC), which represents shape information within a spatial coordinate system [64, 104] and shows increased fMRI responses to noisy face images [62]. However, an important question that remains to be explored is whether it is the FFA or the LOC on whose neural representations the perception of deteriorated and noisy face images is based. Even though combined behavioral and neuroimaging results provided strong evidence for a close link between face perception and the neural processes in the FFA in the case of intact face images [37–40], it has not been investigated whether this holds true also for faces that are noisy and poorly visible.

We have found that adding phase noise to face images leads to reduced and increased fMRI responses to faces in bilateral mid-fusiform gyrus (Fig. 2.3*A*) and bilateral LOC (Fig. 2.3*B*), respectively, which is in agreement with previous results [62, 120]. Importantly, our results provide the first evidence that only in the right face-selective FFA did noise-induced modulation of the fMRI responses show a close association with the individual differences in face identity discrimination performance of noisy faces (Fig. 2.4*B*): smaller decrease of the fMRI responses was associated with better identity discrimination. This relationship was not driven by the overall face perception ability of the participants, because performance for intact faces was regressed out from that for noisy faces. Our results imply that the perception of noisy face images is based on the neural representations extracted from the right FFA.

1.3. I found that the strength of the intrinsic functional connectivity within the visual cortical network composed of bilateral FFA and bilateral object-selective lateral occipital cortex (LOC) predicted the participants' ability to discriminate the identity of noisy face images.

Based on the suggested role of the re-entrant neural mechanisms in the processing of noisy faces, we predicted that the individual ability to handle stimulus noise might depend on the strength of functional interactions between FFA and LOC. To test this prediction, we

estimated the strength of intrinsic functional connectivity between bilateral FFA and LOC (Fig. 2.5*A*) using resting-state fMRI [86] (for review see [87]) and computed correlations between these measures and the face identity discrimination performance for noisy faces. In the correlation analysis the intact face performance was used as a covariate to control for the confounding effect of the overall face perception ability of the participants. Our correlation analysis revealed that the functional connectivity strength between bilateral FFA and bilateral LOC correlated positively with the behavioral accuracy for noisy faces (Fig. 2.5*B*): the stronger the functional connectivity between these regions during rest, the better the face-identity discrimination performance in the noisy condition. These results suggest that face-identity perception in the case of noisy faces is based on functional interactions between bilateral FFA and LOC.

2. **Thesis: I have shown that there is a face-selective repetition-induced fMRIa within the core face-processing network composed of the FFA and OFA which reflects functionally relevant adaptation processes involved in face identity perception.**

Published in [2], [4].

It has been shown that sensory information processing is highly affected by short-term prior perceptual experience. When a sensory stimulus is repeated, the evoked neural signal is invariably smaller than the one observed for its first presentation, an effect termed as repetition suppression (RS) [212]. Similarly, in functional magnetic resonance imaging (fMRI) experiments stimulus repetitions elicit the reduction of the blood oxygenation level-dependent (BOLD) signal when compared to non-repeating stimuli (for a review see [164]), a phenomenon called fMRI adaptation (fMRIa). It has been shown that repetition of identical face stimuli leads to fMRIa in the core face-selective occipitotemporal visual cortical network, involving the bilateral fusiform face area (FFA) and the occipital face area (OFA) [70, 75, 176]. Extensive previous experimental and modeling research has made significant progress in revealing the neural processes involved in RS (for reviews see [165, 169]). However, surprisingly little is known about its behavioral relevance. Therefore, here we aimed at investigating the relationship between fMRIa and face perception ability by measuring in the same human participants both the repetition-induced reduction of fMRI responses in these regions and identity discrimination performance outside the scanner for upright and inverted face stimuli.

2.1. I found a significant fMRIa, i.e. reduced BOLD signal for repeated as compared to alternating faces in the fusiform face area (FFA) and a moderate fMRIa in the occipital face area (OFA). Furthermore, the magnitudes of the face-selective fMRIa measured in these face-processing areas were closely associated.

In agreement with previous results [70, 75, 176], the repetition of identical face stimuli led to significant fMRIa, i.e. reduced BOLD signal in the FFA, and a moderate fMRIa in the OFA, and we also found fMRIa in the extrastriate body area (EBA) for both upright (Fig. 3.4*A*) and inverted (Fig. 3.4*B*) face stimuli. However, it is not known whether fMRIa reflects common or different underlying mechanisms in the tested visual cortical areas. To test this, we calculated pairwise correlations of fMRIa magnitudes among the three regions. In the correlation analysis, the fMRIa for the inverted faces was used as a covariate to control for the individual differences in low-level visual feature adaptation processes. We found a strong correlation of the face-selective fMRIa between OFA and FFA (Fig. 3.6*A*) and also between OFA and EBA (Fig. 3.6*C*), but not between FFA and EBA (Fig. 3.6*B*). These findings imply that fMRIa might involve different components: one is mediated by neural mechanisms that are specific to the core face-processing network and another which affects the fMRI responses in the OFA and EBA, but not in FFA.

2.2. I have shown that the face-selective fMRIa in the two regions of the core face-processing network, namely in the fusiform face area (FFA) and occipital face area (OFA) predicts individual differences in face-selective perceptual ability.

The visual system as an inference machine actively generates and optimizes predictions about the incoming sensory input to make the information processing more efficient as suggested by the predictive coding model of perception [65–68]. From this perspective, RS is a manifestation of minimising prediction error through adaptive changes in predictions. At the neuronal level, RS is generally believed to reflect short-term plastic processes of the neurons, as they adapt to the temporal context of the current environment, presumably as a consequence of dynamic synaptic change within recurrent neural networks (for reviews see [74, 76, 164, 200]). Thereby, RS reflects the flexibility of the neural system and its ability to adjust to continuously changing requirements, optimizing the performance of the individual. We reasoned that if RS (and the consequent fMRIa) indeed reflects the better predictive ability of the neural system then this should manifest on the perceptual level as well: a good generative model of faces can produce better predictions of subsequent stimulation, which leads to better performance and reduced concomitant prediction error unit activity, i.e. fMRIa. To test this prediction, we correlated the individual fMRIa magnitudes measured in the core face-

processing areas, namely the FFA and OFA, as well as in the body-selective EBA with the participants' face identity discrimination perfomance. In the correlation analysis the behavioral and fMRI results for the inverted faces were used as covariates to control for the individual differences in overall object perception ability and basic visual feature adaptation processes, respectively. Our correlation analysis revealed that the magnitude of the fMRIa measured in the FFA (Fig. 3.5*A*) and OFA (Fig. 3.5*B*), but not in the EBA (Fig. 3.5*C*) correlated positively with the behavioral accuracy: the higher the magnitude of the fMRIa for repeated faces, the better the face identity discrimination performance. These results suggest that RS in the core face-processing areas predicts face-selective perceptual ability and thus reflects functionally relevant adaptation processes involved in face identity perception.

6 References

The author's journal publications

[1]   **P. Hermann**, É. M. Bankó, V. Gál, and Z. Vidnyánszky, "Neural basis of identity information extraction from noisy face images," *J. Neurosci.*, vol. 35, no. 18, pp. 7165–7173, May 2015.

[2]   **P. Hermann**, M. Grotheer, G. Kovács, and Z. Vidnyánszky, "The relationship between repetition suppression and face perception," *Brain Imaging Behav.*, pp. 1–11, Jul. 2016.

The author's conference publications

[3]   **P. Hermann**, É. M. Bankó, V. Gál, and Z. Vidnyánszky, "The human face network: insights from intrinsic functional connectivity analysis," presented at the 4th Neuroimaging Workshop, Debrecen, Hungary, 2014, p. 22.

[4]   **P. Hermann**, M. Grotheer, G. Kovács, and Z. Vidnyánszky, "Repetition suppression of fMRI responses in fusiform and occipital face areas predicts individual differences in face perception ability," presented at the 5th Neuroimaging Workshop, Szeged, Hungary, 2015, p. 7.

The author's other journal and conference publications

[5]   C. Amado, **P. Hermann**, P. Kovács, M. Grotheer, Z. Vidnyánszky, and G. Kovács, "The contribution of surprise to the prediction based modulation of fMRI responses," *Neuropsychologia*, vol. 84, pp. 105–112, Apr. 2016.

[6]   M. Grotheer, **P. Hermann**, Z. Vidnyánszky, and G. Kovács, "Repetition probability effects for inverted faces," *NeuroImage*, vol. 102, Part 2, pp. 416–423, Nov. 2014.

[7]   J. Körtvélyes, E. M. Bankó, A. Andics, G. Rudas, J. Németh, **P. Hermann**, and Z. Vidnyánszky, "Visual cortical responses to the input from the amblyopic eye are suppressed during binocular viewing," *Acta Biol. Hung.*, vol. 63 Suppl 1, pp. 65–79, Mar. 2012.

[8]   **P. Hermann**, Á. Kettinger, R. Meszlényi, and Z. Vidnyánszky, "Comparison of the suitability of 32-channel and 64-channel head coils for application in fMRI research," presented at the IBRO Workshop 2016, Budapest, Hungary, 2016.

[9]   A. Catarina, **P. Hermann**, P. Kovács, M. Grotheer, Z. Vidnyánszky, and G. Kovács, "The role of surprise enhancement in predictions," presented at the IBRO Workshop 2016, Budapest, Hungary, 2016.

[10]   P. Kovács, **P. Hermann**, B. Knakker, G. Kovács, and Z. Vidnyánszky, "Uncovering the configural coding of facial information using the face inversion effect," presented at the IBRO Workshop 2016, Budapest, Hungary, 2016.

[11]   **P. Hermann**, M. Grotheer, G. Kovács, and Z. Vidnyánszky, "Resting-state functional connectivity predicts the repetition suppression of fMRI responses in the fusiform gyrus," presented at the 15th Biannual Conference of The Hungarian Neuroscience Society (MITT), Budapest, Hungary, 2015.

[12]   M. Grotheer, Z. Vidnyánszky, **P. Hermann**, and G. Kovács, "Repetition probability effects for inverted faces in the fusiform face area," presented at the 9th PPRU Workshop: Person Perception – From cortical areas to social functions, Jena, Germany, 2014, p. 14.

[13]   **P. Hermann**, V. Gál, É. M. Bankó, and Z. Vidnyánszky, "Resting-state functional connectivity predicts the face selectivity of fMRI responses in the fusiform gyrus," presented at the XIV. Conference of The Hungarian Neuroscience Society (MITT), Budapest, Hungary, 2013, pp. 217–218.

[14]   **P. Hermann**, É. M. Bankó, and Z. Vidnyánszky, "Representation of facial identity information in the medial and anterior temporal lobe," in *Clin. Neurosci.*, vol. 65, no. S1, p. 27, presented at the IBRO Workshop 2012, Szeged, Hungary, 2012.

[15]   **P. Hermann**, "Electrophysiological correlates of object-specific processing deficits in amblyopia," *Pázmány Péter Cathol. Univ. PhD Proc.*, pp. 153–158, 2011.

Publications cited in the dissertation

[16]   B. Duchaine and G. Yovel, "A revised neural framework for face processing," *Annu. Rev. Vis. Sci.*, vol. 1, no. 1, pp. 393–416, Nov. 2015.

[17] G. Yovel, "Neural and cognitive face-selective markers: An integrative review," *Neuropsychologia*, vol. 83, pp. 5–13, Mar. 2016.

[18] R. K. Yin, "Looking at upside-down faces.," *J. Exp. Psychol.*, vol. 81, no. 1, pp. 141–145, Jul. 1969.

[19] J. W. Tanaka and M. J. Farah, "Parts and wholes in face recognition," *Q. J. Exp. Psychol. A*, vol. 46, no. 2, pp. 225–245, May 1993.

[20] M. J. Farah, K. L. Levinson, and K. L. Klein, "Face perception and within-category discrimination in prosopagnosia," *Neuropsychologia*, vol. 33, no. 6, pp. 661–674, Jun. 1995.

[21] M. Moscovitch, G. Winocur, and M. Behrmann, "What is special about face recognition? Nineteen experiments on a person with visual object agnosia and dyslexia but normal face recognition," *J. Cogn. Neurosci.*, vol. 9, no. 5, pp. 555–604, Oct. 1997.

[22] J. V. Haxby, E. A. Hoffman, and M. I. Gobbini, "The distributed human neural system for face perception," *Trends Cogn. Sci.*, vol. 4, no. 6, pp. 223–233, Jun. 2000.

[23] A. Puce, T. Allison, J. C. Gore, and G. McCarthy, "Face-sensitive regions in human extrastriate cortex studied by functional MRI," *J. Neurophysiol.*, vol. 74, no. 3, pp. 1192–1199, Sep. 1995.

[24] N. Kanwisher, J. McDermott, and M. M. Chun, "The fusiform face area: a module in human extrastriate cortex specialized for face perception," *J. Neurosci.*, vol. 17, no. 11, pp. 4302–4311, Jun. 1997.

[25] A. Ishai, C. F. Schmidt, and P. Boesiger, "Face perception is mediated by a distributed cortical network," *Brain Res. Bull.*, vol. 67, no. 1–2, pp. 87–93, Sep. 2005.

[26] D. Y. Tsao, S. Moeller, and W. A. Freiwald, "Comparing face patch systems in macaques and humans," *Proc. Natl. Acad. Sci.*, vol. 105, no. 49, pp. 19514–19519, Dec. 2008.

[27] R. Rajimehr, J. C. Young, and R. B. H. Tootell, "An anterior temporal face patch in human cortex, predicted by macaque maps," *Proc. Natl. Acad. Sci.*, vol. 106, no. 6, pp. 1995–2000, Feb. 2009.

[28] C. J. Fox, G. Iaria, and J. J. S. Barton, "Defining the face processing network: optimization of the functional localizer in fMRI," *Hum. Brain Mapp.*, vol. 30, no. 5, pp. 1637–1651, May 2009.

[29]   K. S. Weiner and K. Grill-Spector, "Sparsely-distributed organization of face and limb activations in human ventral temporal cortex," *NeuroImage*, vol. 52, no. 4, pp. 1559–1573, Oct. 2010.

[30]   B. Rossion, B. Hanseeuw, and L. Dricot, "Defining face perception areas in the human brain: A large-scale factorial fMRI face localizer analysis," *Brain Cogn.*, vol. 79, no. 2, pp. 138–157, Jul. 2012.

[31]   R. McGugin and I. Gauthier, "The reliability of individual differences in face-selective responses in the fusiform gyrus and their relation to face recognition ability," *Brain Imaging Behav.*, pp. 1–12, Nov. 2015.

[32]   E. A. Hoffman and J. V. Haxby, "Distinct representations of eye gaze and identity in the distributed human neural system for face perception," *Nat. Neurosci.*, vol. 3, no. 1, pp. 80–84, Jan. 2000.

[33]   J. S. Winston, R. N. A. Henson, M. R. Fine-Goulden, and R. J. Dolan, "fMRI-adaptation reveals dissociable neural representations of identity and expression in face perception," *J. Neurophysiol.*, vol. 92, no. 3, pp. 1830–1839, Sep. 2004.

[34]   P. Rotshtein, R. N. A. Henson, A. Treves, J. Driver, and R. J. Dolan, "Morphing Marilyn into Maggie dissociates physical and identity face representations in the brain," *Nat. Neurosci.*, vol. 8, no. 1, pp. 107–113, Jan. 2005.

[35]   S. Gilaie-Dotan and R. Malach, "Sub-exemplar shape tuning in human face-related areas," *Cereb. Cortex*, vol. 17, no. 2, pp. 325–338, Feb. 2007.

[36]   A. Nestor, D. C. Plaut, and M. Behrmann, "Unraveling the distributed neural code of facial identity through spatiotemporal pattern analysis," *Proc. Natl. Acad. Sci.*, vol. 108, no. 24, pp. 9998–10003, Jun. 2011.

[37]   K. Grill-Spector, N. Knouf, and N. Kanwisher, "The fusiform face area subserves face perception, not generic within-category identification," *Nat. Neurosci.*, vol. 7, no. 5, pp. 555–562, May 2004.

[38]   N. Furl, L. Garrido, R. Dolan, J. Driver, and B. Duchaine, "Fusiform gyrus face-selectivity reflects facial recognition ability," *J. Cogn. Neurosci.*, vol. 23, no. 7, pp. 1723–1740, Jul. 2011.

[39] L. Huang, Y. Song, J. Li, Z. Zhen, Z. Yang, and J. Liu, "Individual differences in cortical face selectivity predict behavioral performance in face recognition," *Front. Hum. Neurosci.*, vol. 8, p. 483, Jul. 2014.

[40] G. Yovel and N. Kanwisher, "The neural basis of the behavioral face-inversion effect," *Curr. Biol.*, vol. 15, no. 24, pp. 2256–2262, Dec. 2005.

[41] S. L. Fairhall and A. Ishai, "Effective connectivity within the distributed cortical network for face perception," *Cereb. Cortex*, vol. 17, no. 10, pp. 2400–2406, Oct. 2007.

[42] H. Zhang, J. Tian, J. Liu, J. Li, and K. Lee, "Intrinsically organized network for face perception during the resting state," *Neurosci. Lett.*, vol. 454, no. 1, pp. 1–5, Apr. 2009.

[43] J. Davies-Thompson and T. J. Andrews, "Intra- and interhemispheric connectivity between face-selective regions in the human brain," *J. Neurophysiol.*, vol. 108, no. 11, pp. 3087–3095, Dec. 2012.

[44] Z. Zhen, H. Fang, and J. Liu, "The hierarchical brain network for face recognition," *PLoS ONE*, vol. 8, no. 3, p. e59886, Mar. 2013.

[45] J. Liu, A. Harris, and N. Kanwisher, "Stages of processing in face perception: an MEG study," *Nat. Neurosci.*, vol. 5, no. 9, pp. 910–916, Sep. 2002.

[46] S. Hochstein and M. Ahissar, "View from the top: hierarchies and reverse hierarchies in the visual system," *Neuron*, vol. 36, no. 5, pp. 791–804, Dec. 2002.

[47] G. A. Rousselet, M. J.-M. Macé, and M. Fabre-Thorpe, "Is it an animal? Is it a human face? Fast processing in upright and inverted natural scenes," *J. Vis.*, vol. 3, no. 6, p. 5, Jul. 2003.

[48] M. B. Lewis and A. J. Edmonds, "Face detection: mapping human performance," *Perception*, vol. 32, no. 8, pp. 903–920, Aug. 2003.

[49] J. J. DiCarlo and D. D. Cox, "Untangling invariant object recognition," *Trends Cogn. Sci.*, vol. 11, no. 8, pp. 333–341, Aug. 2007.

[50] J. Hegdé, "Time course of visual perception: Coarse-to-fine processing and beyond," *Prog. Neurobiol.*, vol. 84, no. 4, pp. 405–439, Apr. 2008.

[51] S. M. Crouzet, H. Kirchner, and S. J. Thorpe, "Fast saccades toward faces: Face detection in just 100 ms," *J. Vis.*, vol. 10, no. 4, p. 16, Apr. 2010.

[52] J. J. DiCarlo, D. Zoccolan, and N. C. Rust, "How does the brain solve visual object recognition?," *Neuron*, vol. 73, no. 3, pp. 415–434, Feb. 2012.

[53] M. Cauchoix, G. Barragan-Jason, T. Serre, and E. J. Barbeau, "The neural dynamics of face detection in the wild revealed by MVPA," *J. Neurosci.*, vol. 34, no. 3, pp. 846–854, Jan. 2014.

[54] B. Rossion, R. Caldara, M. Seghier, A.-M. Schuller, F. Lazeyras, and E. Mayer, "A network of occipito-temporal face-sensitive areas besides the right middle fusiform gyrus is necessary for normal face processing," *Brain*, vol. 126, no. 11, pp. 2381–2395, Nov. 2003.

[55] B. Rossion, "Constraining the cortical face network by neuroimaging studies of acquired prosopagnosia," *NeuroImage*, vol. 40, no. 2, pp. 423–426, Apr. 2008.

[56] V. Goffaux, J. Peters, J. Haubrechts, C. Schiltz, B. Jansma, and R. Goebel, "From coarse to fine? Spatial and temporal dynamics of cortical face processing," *Cereb. Cortex*, vol. 21, no. 2, pp. 467–476, Feb. 2011.

[57] F. Jiang, L. Dricot, J. Weber, G. Righi, M. J. Tarr, R. Goebel, and B. Rossion, "Face categorization in visual scenes may start in a higher order area of the right fusiform gyrus: evidence from dynamic visual stimulation in neuroimaging," *J. Neurophysiol.*, vol. 106, no. 5, pp. 2720–2736, Nov. 2011.

[58] P. Rotshtein, P. Vuilleumier, J. Winston, J. Driver, and R. Dolan, "Distinct and convergent visual processing of high and low spatial frequency information in faces," *Cereb. Cortex*, vol. 17, no. 11, pp. 2713–2724, Nov. 2007.

[59] J. Steeves, L. Dricot, H. C. Goltz, B. Sorger, J. Peters, A. D. Milner, M. A. Goodale, R. Goebel, and B. Rossion, "Abnormal face identity coding in the middle fusiform gyrus of two brain-damaged prosopagnosic patients," *Neuropsychologia*, vol. 47, no. 12, pp. 2584–2592, Oct. 2009.

[60] D. Pitcher, B. Duchaine, V. Walsh, and N. Kanwisher, "TMS evidence for feedforward and feedback mechanisms of face and body perception," *J. Vis.*, vol. 10, no. 7, pp. 671–671, Aug. 2010.

[61] H. Tang, C. Buia, R. Madhavan, N. E. Crone, J. R. Madsen, W. S. Anderson, and G. Kreiman, "Spatiotemporal dynamics underlying object completion in human ventral visual cortex," *Neuron*, vol. 83, no. 3, pp. 736–748, Aug. 2014.

[62] É. M. Bankó, V. Gál, J. Körtvélyes, G. Kovács, and Z. Vidnyánszky, "Dissociating the effect of noise on sensory processing and overall decision difficulty," *J. Neurosci.*, vol. 31, no. 7, pp. 2663–2674, Feb. 2011.

[63] É. M. Bankó, J. Körtvélyes, B. Weiss, and Z. Vidnyánszky, "How the visual cortex handles stimulus noise: insights from amblyopia," *PLoS ONE*, vol. 8, no. 6, p. e66583, Jun. 2013.

[64] J. Larsson and D. J. Heeger, "Two retinotopic visual areas in human lateral occipital cortex," *J. Neurosci.*, vol. 26, no. 51, pp. 13128–13142, Dec. 2006.

[65] D. Mumford, "On the computational architecture of the neocortex," *Biol. Cybern.*, vol. 66, no. 3, pp. 241–251, Jan. 1992.

[66] R. P. N. Rao and D. H. Ballard, "Predictive coding in the visual cortex: a functional interpretation of some extra-classical receptive-field effects," *Nat. Neurosci.*, vol. 2, no. 1, pp. 79–87, Jan. 1999.

[67] K. Friston, "A theory of cortical responses," *Philos. Trans. R. Soc. Lond. B Biol. Sci.*, vol. 360, no. 1456, pp. 815–836, Apr. 2005.

[68] K. Friston, "The free-energy principle: a unified brain theory?," *Nat. Rev. Neurosci.*, vol. 11, no. 2, pp. 127–138, Feb. 2010.

[69] A. Puce, T. Allison, M. Asgari, J. C. Gore, and G. McCarthy, "Differential sensitivity of human visual cortex to faces, letterstrings, and textures: a functional magnetic resonance imaging study," *J. Neurosci.*, vol. 16, no. 16, pp. 5205–5215, Aug. 1996.

[70] M. P. Ewbank, R. N. Henson, J. B. Rowe, R. S. Stoyanova, and A. J. Calder, "Different neural mechanisms within occipitotemporal cortex underlie repetition suppression across same and different-size faces," *Cereb. Cortex*, vol. 23, no. 5, pp. 1073–1084, May 2013.

[71] H.-J. Park and K. Friston, "Structural and functional brain networks: from connections to cognition," *Science*, vol. 342, no. 6158, p. 1238411, Nov. 2013.

[72] P. Kok and F. P. de Lange, "Predictive coding in sensory cortex," in *An Introduction to Model-Based Cognitive Neuroscience*, B. U. Forstmann and E.-J. Wagenmakers, Eds. Springer New York, 2015, pp. 221–244.

[73] T. H. B. FitzGerald, R. J. Moran, K. J. Friston, and R. J. Dolan, "Precision and neuronal dynamics in the human posterior parietal cortex during evidence accumulation," *NeuroImage*, vol. 107, pp. 219–228, Feb. 2015.

[74] R. Auksztulewicz and K. Friston, "Repetition suppression and its contextual determinants in predictive coding," *Cortex*, vol. 80, pp. 125–140, Jul. 2016.

[75] C. Summerfield, E. H. Trittschuh, J. M. Monti, M.-M. Mesulam, and T. Egner, "Neural repetition suppression reflects fulfilled perceptual expectations," *Nat. Neurosci.*, vol. 11, no. 9, pp. 1004–1006, Sep. 2008.

[76] R. N. A. Henson, "Neuroimaging studies of priming," *Prog. Neurobiol.*, vol. 70, no. 1, pp. 53–81, May 2003.

[77] R. Sayres and K. Grill-Spector, "Object-selective cortex exhibits performance-independent repetition suppression," *J. Neurophysiol.*, vol. 95, no. 2, pp. 995–1007, Feb. 2006.

[78] A. J. Horner and R. N. Henson, "Priming, response learning and repetition suppression," *Neuropsychologia*, vol. 46, no. 7, pp. 1979–1991, Jun. 2008.

[79] S. Gilaie-Dotan, H. Gelbard-Sagiv, and R. Malach, "Perceptual shape sensitivity to upright and inverted faces is reflected in neuronal adaptation," *NeuroImage*, vol. 50, no. 2, pp. 383–395, Apr. 2010.

[80] A. Soldan, C. Habeck, Y. Gazes, and Y. Stern, "Neural mechanisms of repetition priming of familiar and globally unfamiliar visual objects," *Brain Res.*, vol. 1343, pp. 122–134, Jul. 2010.

[81] E. J. Ward, M. M. Chun, and B. A. Kuhl, "Repetition suppression and multi-voxel pattern similarity differentially track implicit and explicit visual memory," *J. Neurosci.*, vol. 33, no. 37, pp. 14749–14757, Sep. 2013.

[82] D. Kaiser, C. Walther, S. R. Schweinberger, and G. Kovács, "Dissociating the neural bases of repetition-priming and adaptation in the human brain for faces," *J. Neurophysiol.*, vol. 110, no. 12, pp. 2727–2738, Dec. 2013.

[83] S. Ogawa, T. M. Lee, A. R. Kay, and D. W. Tank, "Brain magnetic resonance imaging with contrast dependent on blood oxygenation.," *Proc. Natl. Acad. Sci.*, vol. 87, no. 24, pp. 9868–9872, Dec. 1990.

[84] N. K. Logothetis, J. Pauls, M. Augath, T. Trinath, and A. Oeltermann, "Neurophysiological investigation of the basis of the fMRI signal," *Nature*, vol. 412, no. 6843, pp. 150–157, Jul. 2001.

[85] R. A. Poldrack, "Region of interest analysis for fMRI," *Soc. Cogn. Affect. Neurosci.*, vol. 2, no. 1, pp. 67–70, Mar. 2007.

[86] B. Biswal, F. Zerrin Yetkin, V. M. Haughton, and J. S. Hyde, "Functional connectivity in the motor cortex of resting human brain using echo-planar mri," *Magn. Reson. Med.*, vol. 34, no. 4, pp. 537–541, Oct. 1995.

[87] M. D. Fox and M. E. Raichle, "Spontaneous fluctuations in brain activity observed with functional magnetic resonance imaging," *Nat. Rev. Neurosci.*, vol. 8, no. 9, pp. 700–711, Sep. 2007.

[88] M. D. Fox, M. Corbetta, A. Z. Snyder, J. L. Vincent, and M. E. Raichle, "Spontaneous neuronal activity distinguishes human dorsal and ventral attention systems," *Proc. Natl. Acad. Sci.*, vol. 103, no. 26, pp. 10046–10051, Jun. 2006.

[89] J. L. Vincent, G. H. Patel, M. D. Fox, A. Z. Snyder, J. T. Baker, D. C. Van Essen, J. M. Zempel, L. H. Snyder, M. Corbetta, and M. E. Raichle, "Intrinsic functional architecture in the anaesthetized monkey brain," *Nature*, vol. 447, no. 7140, pp. 83–86, May 2007.

[90] V. D. Calhoun, K. A. Kiehl, and G. D. Pearlson, "Modulation of temporally coherent brain networks estimated using ICA at rest and during cognitive tasks," *Hum. Brain Mapp.*, vol. 29, no. 7, pp. 828–838, Jul. 2008.

[91] S. M. Smith, P. T. Fox, K. L. Miller, D. C. Glahn, P. M. Fox, C. E. Mackay, N. Filippini, K. E. Watkins, R. Toro, A. R. Laird, and C. F. Beckmann, "Correspondence of the brain's functional architecture during activation and rest," *Proc. Natl. Acad. Sci.*, vol. 106, no. 31, pp. 13040–13045, Aug. 2009.

[92] A. R. Laird, P. M. Fox, S. B. Eickhoff, J. A. Turner, K. L. Ray, D. R. McKay, D. C. Glahn, C. F. Beckmann, S. M. Smith, and P. T. Fox, "Behavioral interpretations of intrinsic connectivity networks," *J. Cogn. Neurosci.*, vol. 23, no. 12, pp. 4022–4037, Dec. 2011.

[93] M. Mennes, C. Kelly, X.-N. Zuo, A. Di Martino, B. Biswal, F. X. Castellanos, and M. P. Milham, "Inter-individual differences in resting state functional connectivity predict task-induced BOLD activity," *NeuroImage*, vol. 50, no. 4, pp. 1690–1701, May 2010.

[94]   I. Tavor, O. P. Jones, R. B. Mars, S. M. Smith, T. E. Behrens, and S. Jbabdi, "Task-free MRI predicts individual differences in brain activity during task performance," *Science*, vol. 352, no. 6282, pp. 216–220, Apr. 2016.

[95]   M. Hampson, N. R. Driesen, P. Skudlarski, J. C. Gore, and R. T. Constable, "Brain connectivity related to working memory performance," *J. Neurosci.*, vol. 26, no. 51, pp. 13338–13343, Dec. 2006.

[96]   W. W. Seeley, V. Menon, A. F. Schatzberg, J. Keller, G. H. Glover, H. Kenna, A. L. Reiss, and M. D. Greicius, "Dissociable intrinsic connectivity networks for salience processing and executive control," *J. Neurosci.*, vol. 27, no. 9, pp. 2349–2356, Feb. 2007.

[97]   M. Hampson, N. Driesen, J. K. Roth, J. C. Gore, and R. T. Constable, "Functional connectivity between task-positive and task-negative brain areas and its relation to working memory performance," *Magn. Reson. Imaging*, vol. 28, no. 8, pp. 1051–1057, Oct. 2010.

[98]   M. S. Koyama, A. D. Martino, X.-N. Zuo, C. Kelly, M. Mennes, D. R. Jutagir, F. X. Castellanos, and M. P. Milham, "Resting-state functional connectivity indexes reading competence in children and adults," *J. Neurosci.*, vol. 31, no. 23, pp. 8617–8624, Jun. 2011.

[99]   Q. Zhu, J. Zhang, Y. L. L. Luo, D. D. Dilks, and J. Liu, "Resting-state neural activity across face-selective cortical regions is behaviorally relevant," *J. Neurosci.*, vol. 31, no. 28, pp. 10323–10330, Jul. 2011.

[100] A. Baldassarre, C. M. Lewis, G. Committeri, A. Z. Snyder, G. L. Romani, and M. Corbetta, "Individual variability in functional connectivity predicts performance of a perceptual task," *Proc. Natl. Acad. Sci.*, vol. 109, no. 9, pp. 3516–3521, Feb. 2012.

[101] M. W. Cole, T. Yarkoni, G. Repovš, A. Anticevic, and T. S. Braver, "Global connectivity of prefrontal cortex predicts cognitive control and intelligence," *J. Neurosci.*, vol. 32, no. 26, pp. 8988–8999, Jun. 2012.

[102] X. Wang, Z. Han, Y. He, A. Caramazza, L. Song, and Y. Bi, "Where color rests: spontaneous brain activity of bilateral fusiform and lingual regions predicts object color knowledge performance," *NeuroImage*, vol. 76, pp. 252–263, Aug. 2013.

[103] E. B. O'Neil, R. M. Hutchison, D. A. McLean, and S. Köhler, "Resting-state fMRI reveals functional connectivity between face-selective perirhinal cortex and the

fusiform face area related to face inversion," *NeuroImage*, vol. 92, pp. 349–355, May 2014.

[104] E. H. Silson, D. J. McKeefry, J. Rodgers, A. D. Gouws, M. Hymers, and A. B. Morland, "Specialized and independent processing of orientation and shape in visual field maps LO1 and LO2," *Nat. Neurosci.*, vol. 16, no. 3, pp. 267–269, Mar. 2013.

[105] M. D. Fox, A. Z. Snyder, J. L. Vincent, M. Corbetta, D. C. Van Essen, and M. E. Raichle, "The human brain is intrinsically organized into dynamic, anticorrelated functional networks," *Proc. Natl. Acad. Sci.*, vol. 102, no. 27, pp. 9673–9678, Jul. 2005.

[106] B. Tiddeman, M. Burt, and D. Perrett, "Prototyping and transforming facial textures for perception research," *IEEE Comput. Graph. Appl.*, vol. 21, no. 5, pp. 42–50, Sep. 2001.

[107] S. C. Dakin, R. F. Hess, T. Ledgeway, and R. L. Achtman, "What causes non-monotonic tuning of fMRI response to noisy images?," *Curr. Biol.*, vol. 12, no. 14, pp. R476–R477, Jul. 2002.

[108] D. H. Brainard, "The Psychophysics Toolbox," *Spat. Vis.*, vol. 10, no. 4, pp. 433–436, Jan. 1997.

[109] D. G. Pelli, "The VideoToolbox software for visual psychophysics: transforming numbers into movies," *Spat. Vis.*, vol. 10, no. 4, pp. 437–442, Jan. 1997.

[110] J.-M. Geusebroek, G. J. Burghouts, and A. W. M. Smeulders, "The Amsterdam Library of Object Images," *Int. J. Comput. Vis.*, vol. 61, no. 1, pp. 103–112, Jan. 2005.

[111] J. C. Mazziotta, A. W. Toga, A. Evans, P. Fox, and J. Lancaster, "A probabilistic atlas of the human brain: theory and rationale for its development. The International Consortium for Brain Mapping (ICBM)," *NeuroImage*, vol. 2, no. 2, pp. 89–101, Jun. 1995.

[112] J. Mazziotta, A. Toga, A. Evans, P. Fox, J. Lancaster, K. Zilles, R. Woods, T. Paus, G. Simpson, B. Pike, C. Holmes, L. Collins, P. Thompson, D. MacDonald, M. Iacoboni, T. Schormann, K. Amunts, N. Palomero-Gallagher, S. Geyer, L. Parsons, K. Narr, N. Kabani, G. Le Goualher, D. Boomsma, T. Cannon, R. Kawashima, and B. Mazoyer, "A probabilistic atlas and reference system for the human brain: International Consortium for Brain Mapping (ICBM).," *Philos. Trans. R. Soc. Lond. Ser. B*, vol. 356, no. 1412, pp. 1293–1322, Aug. 2001.

[113] J. Mazziotta, A. Toga, A. Evans, P. Fox, J. Lancaster, K. Zilles, R. Woods, T. Paus, G. Simpson, B. Pike, C. Holmes, L. Collins, P. Thompson, D. MacDonald, M. Iacoboni, T. Schormann, K. Amunts, N. Palomero-Gallagher, S. Geyer, L. Parsons, K. Narr, N. Kabani, G. Le Goualher, J. Feidler, K. Smith, D. Boomsma, H. H. Pol, T. Cannon, R. Kawashima, and B. Mazoyer, "A four-dimensional probabilistic atlas of the human brain," *J. Am. Med. Inform. Assoc. JAMIA*, vol. 8, no. 5, pp. 401–430, Oct. 2001.

[114] M. Xia, J. Wang, and Y. He, "BrainNet Viewer: a network visualization tool for human brain connectomics," *PLoS ONE*, vol. 8, no. 7, p. e68910, Jul. 2013.

[115] N. Tzourio-Mazoyer, B. Landeau, D. Papathanassiou, F. Crivello, O. Etard, N. Delcroix, B. Mazoyer, and M. Joliot, "Automated anatomical labeling of activations in SPM using a macroscopic anatomical parcellation of the MNI MRI single-subject brain," *NeuroImage*, vol. 15, no. 1, pp. 273–289, Jan. 2002.

[116] A. Weissenbacher, C. Kasess, F. Gerstl, R. Lanzenberger, E. Moser, and C. Windischberger, "Correlations and anticorrelations in resting-state functional connectivity MRI: A quantitative comparison of preprocessing strategies," *NeuroImage*, vol. 47, no. 4, pp. 1408–1416, Oct. 2009.

[117] D. Cordes, V. M. Haughton, K. Arfanakis, J. D. Carew, P. A. Turski, C. H. Moritz, M. A. Quigley, and M. E. Meyerand, "Frequencies contributing to functional connectivity in the cerebral cortex in 'resting-state' data," *AJNR Am. J. Neuroradiol.*, vol. 22, no. 7, pp. 1326–1333, Aug. 2001.

[118] C. R. Pernet, R. Wilcox, and G. A. Rousselet, "Robust correlation analyses: false positive and power validation using a new open source matlab toolbox," *Front. Psychol.*, vol. 3, p. 606, Jan. 2013.

[119] S. G. Horovitz, B. Rossion, P. Skudlarski, and J. C. Gore, "Parametric design and correlational analyses help integrating fMRI and electrophysiological data during face processing," *NeuroImage*, vol. 22, no. 4, pp. 1587–1595, Aug. 2004.

[120] H. R. Heekeren, S. Marrett, P. A. Bandettini, and L. G. Ungerleider, "A general mechanism for perceptual decision-making in the human brain," *Nature*, vol. 431, no. 7010, pp. 859–862, Oct. 2004.

[121] R. Righart, F. Andersson, S. Schwartz, E. Mayer, and P. Vuilleumier, "Top-down activation of fusiform cortex without seeing faces in prosopagnosia," *Cereb. Cortex*, vol. 20, no. 8, pp. 1878–1890, Aug. 2010.

[122] M. A. Pinsk, M. Arcaro, K. S. Weiner, J. F. Kalkus, S. J. Inati, C. G. Gross, and S. Kastner, "Neural representations of faces and body parts in macaque and human cortex: a comparative fMRI study," *J. Neurophysiol.*, vol. 101, no. 5, pp. 2581–2600, May 2009.

[123] K. Grill-Spector and K. S. Weiner, "The functional architecture of the ventral temporal cortex and its role in categorization," *Nat. Rev. Neurosci.*, vol. 15, no. 8, pp. 536–548, Aug. 2014.

[124] D. Pitcher, V. Walsh, and B. Duchaine, "The role of the occipital face area in the cortical face perception network," *Exp. Brain Res.*, vol. 209, no. 4, pp. 481–493, Apr. 2011.

[125] K. S. Weiner, R. Sayres, J. Vinberg, and K. Grill-Spector, "fMRI-adaptation and category selectivity in human ventral temporal cortex: regional differences across time scales," *J. Neurophysiol.*, vol. 103, no. 6, pp. 3349–3365, Jun. 2010.

[126] Y. Lerner, T. Hendler, D. Ben-Bashat, M. Harel, and R. Malach, "A hierarchical axis of object processing stages in the human visual cortex," *Cereb. Cortex*, vol. 11, no. 4, pp. 287–297, Apr. 2001.

[127] K. Grill-Spector, T. Kushnir, T. Hendler, S. Edelman, Y. Itzchak, and R. Malach, "A sequence of object-processing stages revealed by fMRI in the human occipital lobe," *Hum. Brain Mapp.*, vol. 6, no. 4, pp. 316–328, Jan. 1998.

[128] G. Rainer, M. Augath, T. Trinath, and N. K. Logothetis, "Nonmonotonic noise tuning of BOLD fMRI signal to natural images in the visual cortex of the anesthetized monkey," *Curr. Biol. CB*, vol. 11, no. 11, pp. 846–854, Jun. 2001.

[129] G. Rainer, M. Augath, T. Trinath, and N. K. Logothetis, "The effect of image scrambling on visual cortical BOLD activity in the anesthetized monkey," *NeuroImage*, vol. 16, no. 3, Part A, pp. 607–616, Jul. 2002.

[130] B. S. Tjan, V. Lestou, and Z. Kourtzi, "Uncertainty and invariance in the human visual cortex," *J. Neurophysiol.*, vol. 96, no. 3, pp. 1556–1568, Sep. 2006.

[131] V. P. Clark, R. Parasuraman, K. Keil, R. Kulansky, S. Fannon, J. M. Maisog, L. G. Ungerleider, and J. V. Haxby, "Selective attention to face identity and color studied with fMRI," *Hum. Brain Mapp.*, vol. 5, no. 4, pp. 293–297, Jan. 1997.

[132] E. Wojciulik, N. Kanwisher, and J. Driver, "Covert visual attention modulates face-specific activity in the human fusiform gyrus: fMRI study," *J. Neurophysiol.*, vol. 79, no. 3, pp. 1574–1578, Mar. 1998.

[133] K. M. O'Craven, P. E. Downing, and N. Kanwisher, "fMRI evidence for objects as the units of attentional selection," *Nature*, vol. 401, no. 6753, pp. 584–587, Oct. 1999.

[134] L. Reddy, F. Moradi, and C. Koch, "Top-down biases win against focal attention in the fusiform face area," *NeuroImage*, vol. 38, no. 4, pp. 730–739, Dec. 2007.

[135] A. S. Kayser, D. T. Erickson, B. R. Buchsbaum, and M. D'Esposito, "Neural representations of relevant and irrelevant features in perceptual decision making," *J. Neurosci.*, vol. 30, no. 47, pp. 15778–15789, Nov. 2010.

[136] R. Malach, J. B. Reppas, R. R. Benson, K. K. Kwong, H. Jiang, W. A. Kennedy, P. J. Ledden, T. J. Brady, B. R. Rosen, and R. B. Tootell, "Object-related activity revealed by functional magnetic resonance imaging in human occipital cortex," *Proc. Natl. Acad. Sci.*, vol. 92, no. 18, pp. 8135–8139, Aug. 1995.

[137] K. Grill-Spector, Z. Kourtzi, and N. Kanwisher, "The lateral occipital complex and its role in object recognition," *Vision Res.*, vol. 41, no. 10–11, pp. 1409–1422, May 2001.

[138] U. Hasson, M. Harel, I. Levy, and R. Malach, "Large-scale mirror-symmetry organization of human occipito-temporal object areas," *Neuron*, vol. 37, no. 6, pp. 1027–1041, Mar. 2003.

[139] R. A. Epstein, J. S. Higgins, W. Parker, G. K. Aguirre, and S. Cooperman, "Cortical correlates of face and scene inversion: a comparison," *Neuropsychologia*, vol. 44, no. 7, pp. 1145–1158, 2006.

[140] G. Yovel and N. Kanwisher, "Face Perception: Domain Specific, Not Process Specific," *Neuron*, vol. 44, no. 5, pp. 889–898, Dec. 2004.

[141] P. Rotshtein, J. J. Geng, J. Driver, and R. J. Dolan, "Role of features and second-order spatial-relations in face discrimination, face recognition, and individual face skills," *J. Cogn. Neurosci.*, vol. 19, no. 9, pp. 1435–1452, Sep. 2007.

[142] D. Pitcher, B. Duchaine, V. Walsh, G. Yovel, and N. Kanwisher, "The role of lateral occipital face and object areas in the face inversion effect," *Neuropsychologia*, vol. 49, no. 12, pp. 3448–3453, Oct. 2011.

[143] J. Zhang, X. Li, Y. Song, and J. Liu, "The fusiform face area is engaged in holistic, not parts-based, representation of faces," *PLoS ONE*, vol. 7, no. 7, p. e40390, Jul. 2012.

[144] G. McCarthy, A. Puce, J. C. Gore, and T. Allison, "Face-specific processing in the human fusiform gyrus," *J. Cogn. Neurosci.*, vol. 9, no. 5, pp. 605–610, Oct. 1997.

[145] G. Yovel, A. Tambini, and T. Brandman, "The asymmetry of the fusiform face area is a stable individual characteristic that underlies the left-visual-field superiority for faces," *Neuropsychologia*, vol. 46, no. 13, pp. 3061–3068, Nov. 2008.

[146] D. A. Minnebusch, B. Suchan, O. Köster, and I. Daum, "A bilateral occipitotemporal network mediates face perception," *Behav. Brain Res.*, vol. 198, no. 1, pp. 179–185, Mar. 2009.

[147] B. Mohr, A. Landgrebe, and S. R. Schweinberger, "Interhemispheric cooperation for familiar but not unfamiliar face processing," *Neuropsychologia*, vol. 40, no. 11, pp. 1841–1848, 2002.

[148] S. R. Schweinberger, L. M. Baird, M. Blümler, J. M. Kaufmann, and B. Mohr, "Interhemispheric cooperation for face recognition but not for affective facial expressions," *Neuropsychologia*, vol. 41, no. 4, pp. 407–414, 2003.

[149] J. Reinholz and S. Pollmann, "Neural basis of redundancy effects in visual object categorization," *Neurosci. Lett.*, vol. 412, no. 2, pp. 123–128, Jan. 2007.

[150] L. M. Baird and A. M. Burton, "The bilateral advantage for famous faces: Interhemispheric communication or competition?," *Neuropsychologia*, vol. 46, no. 5, pp. 1581–1587, Apr. 2008.

[151] B. Rossion, L. Dricot, A. Devolder, J. M. Bodart, M. Crommelinck, B. De Gelder, and R. Zoontjes, "Hemispheric asymmetries for whole-based and part-based face processing in the human fusiform gyrus," *J. Cogn. Neurosci.*, vol. 12, no. 5, pp. 793–802, Sep. 2000.

[152] J. S. Lobmaier, P. Klaver, T. Loenneker, E. Martin, and F. W. Mast, "Featural and configural face processing strategies: evidence from a functional magnetic resonance imaging study:," *NeuroReport*, vol. 19, no. 3, pp. 287–291, Feb. 2008.

[153] A. Harris and G. K. Aguirre, "Neural tuning for face wholes and parts in human fusiform gyrus revealed by fMRI adaptation," *J. Neurophysiol.*, vol. 104, no. 1, pp. 336–345, Jul. 2010.

[154] M. Meng, T. Cherian, G. Singal, and P. Sinha, "Lateralization of face processing in the human brain," *Proc. R. Soc. B Biol. Sci.*, vol. 279, no. 1735, pp. 2052–2061, May 2012.

[155] T. Tanskanen, R. Näsänen, T. Montez, J. Päällysaho, and R. Hari, "Face recognition and cortical responses show similar sensitivity to noise spatial frequency," *Cereb. Cortex*, vol. 15, no. 5, pp. 526–534, May 2005.

[156] G. C. Baylis and E. T. Rolls, "Responses of neurons in the inferior temporal cortex in short term and serial recognition memory tasks," *Exp. Brain Res.*, vol. 65, no. 3, pp. 614–622, Feb. 1987.

[157] E. K. Miller, P. M. Gochin, and C. G. Gross, "Habituation-like decrease in the responses of neurons in inferior temporal cortex of the macaque," *Vis. Neurosci.*, vol. 7, no. 4, pp. 357–362, Oct. 1991.

[158] E. K. Miller, L. Li, and R. Desimone, "A neural mechanism for working and recognition memory in inferior temporal cortex," *Science*, vol. 254, no. 5036, pp. 1377–1379, Nov. 1991.

[159] S. Sobotka and J. L. Ringo, "Stimulus specific adaptation in excited but not in inhibited cells in inferotemporal cortex of macaque," *Brain Res.*, vol. 646, no. 1, pp. 95–99, May 1994.

[160] J. L. Ringo, "Stimulus specific adaptation in inferior temporal and medial temporal cortex of the monkey," *Behav. Brain Res.*, vol. 76, no. 1–2, pp. 191–197, Apr. 1996.

[161] H. Sawamura, G. A. Orban, and R. Vogels, "Selectivity of neuronal adaptation does not match response selectivity: a single-cell study of the fMRI adaptation paradigm," *Neuron*, vol. 49, no. 2, pp. 307–318, Jan. 2006.

[162] D. A. Kaliukhovich and R. Vogels, "Stimulus repetition probability does not affect repetition suppression in macaque inferior temporal cortex," *Cereb. Cortex*, vol. 21, no. 7, pp. 1547–1558, Jul. 2011.

[163] D. A. Kaliukhovich and R. Vogels, "Stimulus repetition affects both strength and synchrony of macaque inferior temporal cortical activity," *J. Neurophysiol.*, vol. 107, no. 12, pp. 3509–3527, Jun. 2012.

[164] R. N. A. Henson and M. D. Rugg, "Neural response suppression, haemodynamic repetition effects, and behavioural priming," *Neuropsychologia*, vol. 41, no. 3, pp. 263–270, 2003.

[165] K. Grill-Spector, R. Henson, and A. Martin, "Repetition and the brain: neural models of stimulus-specific effects," *Trends Cogn. Sci.*, vol. 10, no. 1, pp. 14–23, Jan. 2006.

[166] R. Vogels, "Sources of adaptation of inferior temporal cortical responses," *Cortex*, vol. 80, pp. 185–195, Jul. 2016.

[167] G. Kovács and R. Vogels, "When does repetition suppression depend on repetition probability?," *Front. Hum. Neurosci.*, vol. 8, p. 685, Sep. 2014.

[168] M. Grotheer and G. Kovács, "Can predictive coding explain repetition suppression?," *Cortex*, vol. 80, pp. 113–124, Jul. 2016.

[169] N. Bunzeck and C. Thiel, "Neurochemical modulation of repetition suppression and novelty signals in the human brain," *Cortex*, vol. 80, pp. 161–173, Jul. 2016.

[170] A. J. Horner and R. N. Henson, "Repetition suppression in occipitotemporal cortex despite negligible visual similarity: Evidence for postperceptual processing?," *Hum. Brain Mapp.*, vol. 32, no. 10, pp. 1519–1534, Oct. 2011.

[171] S. Magnussen, "Low-level memory processes in vision," *Trends Neurosci.*, vol. 23, no. 6, pp. 247–251, Jun. 2000.

[172] T. Ganel, C. L. R. Gonzalez, K. F. Valyear, J. C. Culham, M. A. Goodale, and S. Köhler, "The relationship between fMRI adaptation and repetition priming," *NeuroImage*, vol. 32, no. 3, pp. 1432–1440, Sep. 2006.

[173] C. Schiltz, B. Sorger, R. Caldara, F. Ahmed, E. Mayer, R. Goebel, and B. Rossion, "Impaired face discrimination in acquired prosopagnosia is associated with abnormal response to individual faces in the right middle fusiform gyrus," *Cereb. Cortex*, vol. 16, no. 4, pp. 574–586, Apr. 2006.

[174] J. Jonas, B. Rossion, J. Krieg, L. Koessler, S. Colnat-Coulbois, H. Vespignani, C. Jacques, J.-P. Vignal, H. Brissart, and L. Maillard, "Intracerebral electrical stimulation of a face-selective area in the right inferior occipital cortex impairs individual face discrimination," *NeuroImage*, vol. 99, pp. 487–497, Oct. 2014.

[175] P. E. Downing, Y. Jiang, M. Shuman, and N. Kanwisher, "A cortical area selective for visual processing of the human body," *Science*, vol. 293, no. 5539, pp. 2470–2473, Sep. 2001.

[176] G. Kovács, L. Iffland, Z. Vidnyánszky, and M. W. Greenlee, "Stimulus repetition probability effects on repetition suppression are position invariant for faces," *NeuroImage*, vol. 60, no. 4, pp. 2128–2135, May 2012.

[177] G. Kovács, D. Kaiser, D. A. Kaliukhovich, Z. Vidnyánszky, and R. Vogels, "Repetition probability does not affect fMRI repetition suppression for objects," *J. Neurosci.*, vol. 33, no. 23, pp. 9805–9812, Jun. 2013.

[178] A. Trujillo-Ortiz, R. Hernandez-Walls, K. Barba-Rojo, and L. Cupul-Magana, "HZmvntest: Henze–Zirkler's Multivariate Normality Test.," 2007. [A MATLAB file] Available:

http://www.mathworks.com/matlabcentral/fileexchange/loadFile.do?objectId=17931

[179] G. Y. Zou, "Toward using confidence intervals to compare correlations," *Psychol. Methods*, vol. 12, no. 4, pp. 399–413, Dec. 2007.

[180] J. S. Winston, R. N. A. Henson, M. R. Fine-Goulden, and R. J. Dolan, "fMRI-adaptation reveals dissociable neural representations of identity and expression in face perception," *J. Neurophysiol.*, vol. 92, no. 3, pp. 1830–1839, Sep. 2004.

[181] T. J. Andrews and M. P. Ewbank, "Distinct representations for facial identity and changeable aspects of faces in the human temporal lobe," *NeuroImage*, vol. 23, no. 3, pp. 905–913, Nov. 2004.

[182] J. Larsson and A. T. Smith, "fMRI repetition suppression: neuronal adaptation or stimulus expectation?," *Cereb. Cortex*, vol. 22, no. 3, pp. 567–576, Mar. 2012.

[183] H. Hecaen and R. Angelergues, "Agnosia for faces (prosopagnosia)," *Arch. Neurol.*, vol. 7, pp. 92–100, Aug. 1962.

[184] J. C. Meadows, "The anatomical basis of prosopagnosia," *J. Neurol. Neurosurg. Psychiatry*, vol. 37, no. 5, pp. 489–501, May 1974.

[185] D. Pitcher, V. Walsh, G. Yovel, and B. Duchaine, "TMS evidence for the involvement of the right occipital face area in early face processing," *Curr. Biol.*, vol. 17, no. 18, pp. 1568–1573, Sep. 2007.

[186] K. Nagy, M. W. Greenlee, and G. Kovács, "The lateral occipital cortex in the face perception network: an effective connectivity study," *Front. Psychol.*, vol. 3, p. 141, May 2012.

[187] M. Gschwind, G. Pourtois, S. Schwartz, D. V. D. Ville, and P. Vuilleumier, "White-matter connectivity between face-responsive regions in the human brain," *Cereb. Cortex*, vol. 22, no. 7, pp. 1564–1576, Jul. 2012.

[188] Y. Liu, S. O. Murray, and B. Jagadeesh, "Time course and stimulus dependence of repetition-induced response suppression in inferotemporal cortex," *J. Neurophysiol.*, vol. 101, no. 1, pp. 418–436, Jan. 2009.

[189] W. D. Baene and R. Vogels, "Effects of adaptation on the stimulus selectivity of macaque inferior temporal spiking activity and local field potentials," *Cereb. Cortex*, vol. 20, no. 9, pp. 2145–2165, Sep. 2010.

[190] M. Spiridon, B. Fischl, and N. Kanwisher, "Location and spatial profile of category-specific regions in human extrastriate cortex," *Hum. Brain Mapp.*, vol. 27, no. 1, pp. 77–89, Jan. 2006.

[191] M. A. Pinsk, M. Arcaro, K. S. Weiner, J. F. Kalkus, S. J. Inati, C. G. Gross, and S. Kastner, "Neural representations of faces and body parts in macaque and human cortex: a comparative fMRI study," *J. Neurophysiol.*, vol. 101, no. 5, pp. 2581–2600, May 2009.

[192] K. Grill-Spector, T. Kushnir, T. Hendler, and R. Malach, "The dynamics of object-selective activation correlate with recognition performance in humans," *Nat. Neurosci.*, vol. 3, no. 8, pp. 837–843, Aug. 2000.

[193] A. Nestor, J. M. Vettel, and M. J. Tarr, "Task-specific codes for face recognition: how they shape the neural representation of features for detection and individuation," *PLoS ONE*, vol. 3, no. 12, p. e3978, Dec. 2008.

[194] S. Nasr and R. B. Tootell, "Role of fusiform and anterior temporal cortical areas in facial recognition," *NeuroImage*, vol. 63, no. 3, pp. 1743–1753, Nov. 2012.

[195] J. O. Goh, A. Suzuki, and D. C. Park, "Reduced neural selectivity increases fMRI adaptation with age during face discrimination," *NeuroImage*, vol. 51, no. 1, pp. 336–344, May 2010.

[196] X. Jiang, A. Bollich, P. Cox, E. Hyder, J. James, S. A. Gowani, N. Hadjikhani, V. Blanz, D. S. Manoach, J. J. S. Barton, W. D. Gaillard, and M. Riesenhuber, "A quantitative link between face discrimination deficits and neuronal selectivity for faces in autism," *NeuroImage Clin.*, vol. 2, pp. 320–331, Feb. 2013.

[197] G. Avidan, U. Hasson, R. Malach, and M. Behrmann, "Detailed exploration of face-related processing in congenital prosopagnosia: 2. Functional neuroimaging findings," *J. Cogn. Neurosci.*, vol. 17, no. 7, pp. 1150–1167, Jul. 2005.

[198] L. M. Solomon-Harris, C. R. Mullin, and J. K. E. Steeves, "TMS to the 'occipital face area' affects recognition but not categorization of faces," *Brain Cogn.*, vol. 83, no. 3, pp. 245–251, Dec. 2013.

[199] H. Yang, T. Susilo, and B. Duchaine, "The anterior temporal face area contains invariant representations of face identity that can persist despite the loss of right FFA and OFA," *Cereb. Cortex*, vol. 26, no. 3, pp. 1096–1107, Mar. 2016.

[200] R. N. Henson, "Repetition suppression to faces in the fusiform face area: A personal and dynamic journey," *Cortex*, vol. 80, pp. 174–184, Jul. 2016.

[201] P. Sinha, B. Balas, Y. Ostrovsky, and R. Russell, "Face recognition by humans: Nineteen results all computer vision researchers should know about," *Proc. IEEE*, vol. 94, no. 11, pp. 1948–1962, Nov. 2006.

[202] N. Weiskopf, "Real-time fMRI and its application to neurofeedback," *NeuroImage*, vol. 62, no. 2, pp. 682–692, Aug. 2012.

[203] R. T. Thibault, M. Lifshitz, and A. Raz, "The self-regulating brain and neurofeedback: Experimental science and clinical promise," *Cortex*, vol. 74, pp. 247–261, Jan. 2016.

[204] K. Shibata, T. Watanabe, Y. Sasaki, and M. Kawato, "Perceptual learning incepted by decoded fMRI neurofeedback without stimulus presentation," *Science*, vol. 334, no. 6061, pp. 1413–1415, Dec. 2011.

[205] F. Scharnowski, C. Hutton, O. Josephs, N. Weiskopf, and G. Rees, "Improving visual perception through neurofeedback," *J. Neurosci.*, vol. 32, no. 49, pp. 17830–17841, Dec. 2012.

[206] Y. Koush, M. J. Rosa, F. Robineau, K. Heinen, S. W Rieger, N. Weiskopf, P. Vuilleumier, D. Van De Ville, and F. Scharnowski, "Connectivity-based neurofeedback: dynamic causal modeling for real-time fMRI," *NeuroImage*, vol. 81, pp. 422–430, Nov. 2013.

[207] F. Robineau, S. W. Rieger, C. Mermoud, S. Pichon, Y. Koush, D. Van De Ville, P. Vuilleumier, and F. Scharnowski, "Self-regulation of inter-hemispheric visual cortex

balance through real-time fMRI neurofeedback training," *NeuroImage*, vol. 100, pp. 1–14, Oct. 2014.

[208] M. Ramot, S. Grossman, D. Friedman, and R. Malach, "Covert neurofeedback without awareness shapes cortical network spontaneous connectivity," *Proc. Natl. Acad. Sci.*, vol. 113, no. 17, pp. E2413–E2420, Apr. 2016.

[209] G. Avidan, M. Tanzer, F. Hadj-Bouziane, N. Liu, L. G. Ungerleider, and M. Behrmann, "Selective dissociation between core and extended regions of the face processing network in congenital prosopagnosia," *Cereb. Cortex*, vol. 24, no. 6, pp. 1565–1578, Jun. 2014.

[210] Y. Song, Q. Zhu, J. Li, X. Wang, and J. Liu, "Typical and atypical development of functional connectivity in the face network," *J. Neurosci.*, vol. 35, no. 43, pp. 14624–14635, Oct. 2015.

[211] M. Lohse, L. Garrido, J. Driver, R. J. Dolan, B. C. Duchaine, and N. Furl, "Effective connectivity from early visual cortex to posterior occipitotemporal face areas supports face selectivity and predicts developmental prosopagnosia," *J. Neurosci.*, vol. 36, no. 13, pp. 3821–3828, Mar. 2016.

[212] R. Desimone, "Neural mechanisms for visual memory and their role in attention," *Proc. Natl. Acad. Sci.*, vol. 93, no. 24, pp. 13494–13499, Nov. 1996.